

**ARTIFICIAL INTELLIGENCE MODEL TO ASSIST
AND EVALUATE THE KIDNEY STONE ON
COMPUTED TOMOGRAPHY IMAGE**

**A THESIS SUBMITTED TO THE GRADUATE
SCHOOL OF APPLIED SCIENCES
OF
NEAR EAST UNIVERSITY**

**By
ÖZLEM SABUNCU**

**In Partial Fulfillment of the Requirements for the
Degree of Master of Science in
Electrical and Electronics Engineering**

NICOSIA, 2021

**ÖZLEM
SABUNCU**

**ARTIFICIAL INTELLIGENCE MODEL TO ASSIST AND
EVALUATE THE KIDNEY STONE ON COMPUTED TOMOGRAPHY IMAGE**

**NEU
2021**

**ARTIFICIAL INTELLIGENCE MODEL TO ASSIST
AND EVALUATE THE KIDNEY STONE ON
COMPUTED TOMOGRAPHY IMAGE**

**A THESIS SUBMITTED TO THE GRADUATE
SCHOOL OF APPLIED SCIENCES
OF
NEAR EAST UNIVERSITY**

**By
ÖZLEM SABUNCU**

**In Partial Fulfillment of the Requirements for the
Degree of Master of Science in
Electrical and Electronics Engineering**

NICOSIA, 2021

**Özlem SABUNCU: ARTIFICIAL INTELLIGENCE MODEL TO ASSIST AND
EVALUATE THE KIDNEY STONE ON COMPUTED TOMOGRAPHY IMAGE**

Institute of Graduate Studies Approval

Prof. Dr. K. Hüsnü Can BAŞER

**We certify this thesis is satisfactory for the award of the degree of Masters of Science
in Electrical and Electronics Engineering**

Examining Committee in Charge:

Prof. Dr. Bülent Bilgehan

Thesis Supervisor: Department of Electrical
and Electronics Engineering, NEU



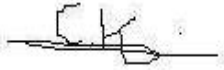
Assist. Prof. Dr. Parvaneh Esmaili

Department of Electrical and Electronics
Engineering, NEU



Assist. Prof. Dr. Cemal Kavalcıoğlu

Department of Electrical and Electronics
Engineering, NEU



I hereby declare that all information in this document has been obtained and presented in accordance with academic rules and ethical conduct. I also declare that, as required by these rules and conduct, I have fully cited and referenced all material and results that are not original to this work.

Name, Last name: Özlem Sabuncu

Signature: 

Date: 21.06.2021

ACKNOWLEDGEMENTS

Foremost, I would like to thank my thesis advisor Prof. Dr. Bülent Bilgehan for his valuable ideas and guidance, for his support and tolerance for the completion of my thesis, during this process from the formation of the thesis to the completion of the thesis.

I especially want to thank my dear family, parents, brother, and sister: I owe you all my success. Thank you for your unconditional love and support. Thank you very much for your support, belief in me, and for being with me in every step of my life throughout my education life. Your presence by my side has always been the main reason for my success.

During this process, I would like to thank Omid Mirzaei, Şerife Kaba, and Ali Işın, who patiently and attentively helped me and supported me whenever I consulted, and especially Özlem Tanrıkulu and all my friends who have always supported me.

To my parents...

ABSTRACT

Stone formation in the kidneys is a common disease, the high rate of recurrence and morbidity of the disease worries all patient groups with kidney stones. There are many imaging options for the diagnosis and management of kidney stone disease, computed tomography (CT) imaging is the preferred method. Radiologists need to analyse large numbers of CT slices manually in order to diagnose kidney stones. This process is laborious and time-consuming. Radiologists analyse CT images by eye ball estimation, because of the manual analysis human errors can be occurred.

In this study, deep learning algorithms were used for the analysis of kidney stones. Convolutional neural network architectures based on deep learning are a preferred method especially for analyzing medical images. High performances can be achieved with deep learning, especially for the analysis of data obtained from advanced scanners such as CT, which provide high-dimensional medical images. The main purpose of this study is to classify kidney stones with high accuracy from CT scans using deep learning algorithms. In this study, selected and pre-trained Convolutional neural network (CNN) architectures were applied to a dataset of abdominal CT scans of patients with kidney stones labeled by a radiologist. As a result of the tests performed with the selected 5 different CNN models, it was observed that these models achieved acceptable performance for kidney stone classification task.

Keywords: Kidney Stone; Computed Tomography; Artificial Intelligence; Deep Learning; Convolutional Neural Network

ÖZET

Böbreklerde taş oluşumu yaygın bir hastalıktır, hastalığın nüks oranının yüksek olması ve morbidite oranı böbrek taşına sahip tüm hasta gruplarını endişelendirir. Böbrek taşı hastalığının tanı ve yönetimi için birçok görüntüleme seçeneği vardır, bilgisayarlı görüntüleme (BT) tercih edilen bir yöntemdir. Radyologların böbrek taşlarını teşhis etmek için çok sayıda BT kesitini manuel olarak analiz etmesi gerekir. Bu süreç zahmetli ve zaman alıcıdır. Radyologlar BT görüntülerini göz kararı tahmini ile analiz eder, manuel analiz nedeniyle insan hataları meydana gelebilir.

Bu çalışmada böbrek taşlarının analizi için derin öğrenme algoritmalarına başvurulmuştur. Derin öğrenme tabanlı olan evrişimli sinir ağı mimarileri, özellikle tıbbi görüntüleri analiz etmek için tercih edilen bir yöntemdir. Özellikle yüksek boyutlu tıbbi görüntüler sağlayan BT gibi gelişmiş tarayıcılardan elde edilen verilerin analizi için derin öğrenme ile yüksek performanslar elde edilebilir. Bu çalışmanın temel amacı, derin öğrenme algoritmalarını kullanarak böbrek taşlarını BT taramalarından, yüksek doğruluk oranı ile sınıflandırmaktır. Bu çalışmada seçilen ve önceden eğitilmiş evrişimli sinir ağı (ESA) mimarileri, radyolog tarafından etiketlenen böbrek taşına sahip hastaların abdominal BT taramalarından oluşan bir veri setine uygulanmıştır. Seçilen 5 farklı ESA modeli ile yapılan testler sonucunda böbrek taşı sınıflandırılması için bu modellerin kabul edilebilir performans elde ettikleri gözlemlenmiştir.

Anahtar kelimeler: Böbrek Taşı; Bilgisayarlı Tomografi; Yapay Zeka; Derin Öğrenme; Evrişimli Sinir Ağı

TABLE OF CONTENTS

ACKNOWLEDGEMENTS	ii
ABSTRACT	iv
ÖZET	v
TABLE OF CONTENTS	vi
LIST OF TABLES	viii
LIST OF FIGURES	ix
LIST OF ABBREVIATIONS	x

CHAPTER 1: INTRODUCTION

1.1 Thesis Problem	2
1.2 Aims of the Study	3
1.3 Significance of the Study	3
1.4 Overview of the Thesis	3

CHAPTER 2: LITERATURE REVIEW

 4

CHAPTER 3: CLINICAL BACKGROUND

3.1 Kidney	9
3.2 Kidney Stone	11
3.2.1 Epidemiology	12
3.2.2 Kidney stone creation	13
3.2.3 Sites of stone growth	13
3.2.4 Stone types	14
3.2.5 Risk factors for kidney stone creation	15
3.3 Kidney Stone Imaging	16
3.3.1 Noncontrast computed tomography	17

3.3.2 Ultrasonography (USG).....	21
3.3.3 Kidney ureter bladder radiography (KUB).....	23
3.3.4 Magnetic resonance imaging (MRI).....	24
3.3.5 Intravenous urography (IVU)	24
CHAPTER 4: CNN’S APPLICATION IN KIDNEY STONE ANALYSIS	
4.1 Deep Learning	26
4.2 Convolutional Neural Network	28
4.2.1 AlexNet.....	38
4.2.2 ResNet-101	38
4.2.3 Inception-V3.....	42
4.2.4 EfficientNet-B0	45
4.2.5 NasNet-Mobile	48
4.3 Database	50
4.4 Algorithm of the Applied Methods.....	52
CHAPTER 5: RESULTS	54
CHAPTER 6: CONCLUSION	56
REFERENCES	58
APPENDICES	71
APPENDIX: VARIOUS CT IMAGES	72

LIST OF TABLES

Table 4.1: Dataset	50
Table 4.2: Dataset and data division.....	52
Table 5.1: Performance Results.....	54

LIST OF FIGURES

Figure 3.1: The Human Kidney.....	9
Figure 3.2: (A) Healthy Kidney, (B) Kidney with Kidney Stones.....	11
Figure 3.3: Imaging of kidney stone with non-contrast CT	17
Figure 3.4: (A) Axial and (B) Coronal non-contrast CT images.....	18
Figure 3.5: (A) Axial Kidney Image, (B) Color-Coded Map Used Image.....	21
Figure 3.6: A stone was identified with the sagittal view of the left kidney	22
Figure 4.1: (A) Deep Learning Neural Network, (B) Artificial Neural Network	27
Figure 4.2: Architecture of CNN.....	29
Figure 4.3: Structure of a typical CNN	30
Figure 4.4: Convolution Process	31
Figure 4.5: Maximum Pooling Process	33
Figure 4.6: Fully Connected Layer.....	33
Figure 4.7: Dropout Function.....	34
Figure 4.8: Structures of the AlexNet.....	35
Figure 4.9: AlexNet Architecture	36
Figure 4.10: ResNet-101 Architecture	39
Figure 4.11: Shortcut connections of ResNet-101	40
Figure 4.12: Inception-V3 Network Architecture	43
Figure 4.13: An architecture of the Inception-V3 module	43
Figure 4.14: Architecture of Inception-V3	45
Figure 4.15: The EfficientNet-B0 Network Architecture.....	46
Figure 4.16: EfficientNet-B0 Network Model	48
Figure 4.17: NASNet Architecture.....	48
Figure 4.18: Images of database, CT abdominal patient samples	51

LIST OF ABBREVIATIONS

ANN:	Artificial Neural Network
BMI:	Body Mass Index
CPU:	Central Processing Unit
CT:	Computed Tomography
DECT:	Dual Energy CT
DL:	Deep Learning
DNN:	Deep Neural Network
ECF:	Extracellular Fluid
FLOPS:	Floating Point Operations Per Second
GFR:	Glomerular Filtration Rate
HU:	Hounsfield Unit
ILSVRC:	ImageNet Large-Scale Visual Recognition Challenge
IVU:	Intravenous Urography
KUB:	Kidney, Ureter, Bladder
MAC:	Multi-Accumulates Cells
MBCConv:	Mobile Inverted Bottleneck Convolution
MDCT:	Multiple Detector CT
ML:	Machine Learning
MRI:	Magnetic Resonance Imaging
NAS:	Neural Architecture Search
PCNL:	Percutaneous Nephrolithotomy
ReLU:	Rectified Linear Units Layer
RNN:	Recurrent Neural Network
SGD:	Stochastic Gradient Descent

SWL: Shock Wave Lithotripsy
TE: Echo Times
USG: Ultrasonography
VOI: Volume Of Interest
WHO: World Health Organization

CHAPTER 1

INTRODUCTION

Kidney stone disease is the appearance of stone-like acid salts and mineral deposits in the kidneys. When these substances are above the saturation point in the urine, concretization may occur in the kidneys (Waldman, 2019). It is an increasing urinary system disease of human health and it is known to affect approximately 12% of the world population (Alealign and Petros, 2018). Kidney stone disease, which is thought to have increased in the last few decades, is a common problem affecting 1 in 10 people (McCarthy et al., 2016). The increase in the incidence of kidney stones is associated with factors such as changes in diet, obesity levels, genetic predisposition, drugs used, and geography (Milenkovic and Albersen, 2019). Nephrolithiasis means stone formation in the collecting ducts of the kidneys or renal tubules. Most of the kidney stone compositions are calcium-based. It is seen in asymptomatic small stones compared to obstructive stones that impair kidney functions and cause the disease to become chronic. The severity of kidney stone disease, together with the pathogenesis, depends on the location of the stone, the composition of the stone, and the size of the stone (Monk and Bushinsky, 2010).

Imaging the kidneys is an important element in the management of kidney stone disease (Rao, 2004). Imaging of nephrolithiasis is of vital importance in the diagnosis, treatment, and follow-up of the disease. The selected imaging method can provide the necessary information about the anatomical, physiological and functional structures of the kidneys (Dhar and Denstedt, 2009). The choice of imaging modality to evaluate abnormalities of the kidneys depends on the amount of radiation, cost, complications that may occur, and ability to diagnose (Kaur and Juneja, 2018). Many diagnostic and therapeutic data can be obtained by imaging the kidneys. These data are important for stone detection, determination of stone burden and distribution in the kidney, understanding the function of the kidney, creating a treatment plan, and understanding the results of treatment (Rao, 2004).

Imaging methods available to view nephrolithiasis include computed tomography (CT), ultrasonography (USG), kidney, ureter, bladder (KUB) radiography, and magnetic resonance imaging (MRI) (Brisbane et al., 2016). Imaging methods used to detect kidney

stones have changed over time. Instead of the intravenous pyelogram (IVP) and KUB films, which were used frequently before, non-contrast CT and USG are used more frequently today (Pfau and Knauf, 2016). In patients with kidney stones, non-contrast CT is often used to scan the kidneys. Kidney stones have different compositions and therefore absorb much radiation and can be easily imaged without requiring contrast (Brisbane et al., 2016).

Deep learning (DL) is a sub-branch of machine learning (ML) and is used in many areas such as medical image processing and computer vision. Convolutional neural networks (CNNs), one of the deep learning algorithms, are seen as the center of deep learning for processing medical images (Pacal et al., 2020). A CNN has a deep architecture and thus is successful at extracting distinctive features (Tajbakhsh et al., 2016). CNNs are used in image recognition tasks. These are used for many tasks including image classification, segmentation, detection (Ker et al., 2017).

Since DL algorithms are successful in image analysis, they have a high potential in the field of radiology. DL algorithms are capable of reaching a repeatable result in less time than it takes for a person to make an assessment. It also has the potential to evaluate a large number of features, including those that have been overlooked by radiologists (Mazurowski et al., 2019).

In this study, deep learning algorithms will be used to classify kidney stones using a CT database. Five different CNN models will be used, which is the main method of deep learning.

1.1 Thesis Problem

Kidney stone disease is increasing in global prevalence and recurrence rate due to limited drug options. It is a disease that affects all ages and genders. (Alelign and Petros, 2018).

The first step in determining kidney stone disease is imaging. There are different imaging options. Radiologists need to manually scan multiple image slices to analyze kidney stones from CT images. At this stage, overlooked situations may occur. Also, the repeatability of manual methods is time-consuming.

1.2 Aims of the Study

Radiologists manually classify kidney stones. There is a need for automatic classification and detection of kidney stones. Therefore, this study aims to use powerful deep networks for the classification of kidney stones.

- To use deep learning methods to classify kidney stones on CT images.
- Achieving high success rates with deep learning-based CNN models.

1.3 Significance of the Study

The findings obtained as a result of this study will provide information about whether there are stones in the kidneys.

This study will provide useful information during the processes such as diagnosis, treatment, and surgical operation of patients with kidney stones.

It contributes to the reduction of errors such as human errors in manual scanning of CT images.

1.4 Overview of the Thesis

Chapter 1 is an introductory chapter of the whole thesis work, outlining the thesis problem, aim of the study, significance of the research. Chapter 2 is a detailed clinical background of the kidney, including the kidney stone, kidney stone imaging methods. Chapter 3 is a literature review of previous studies carried out and related to the present research. Chapter 4 outlines the deep learning-based CNN methods used for the analysis of kidney stones and the application of these methods to CT images. Chapter 5 is the results of the analysis; the conclusion is contained in chapter 6.

CHAPTER 2

LITERATURE REVIEW

Researchers can analyze and understand complex phenomena from engineering, medicine, biology, and various other fields with machine learning. New paradigms are needed to analyze these increasingly complex areas and transform them into useful information for medical services. There has been a tendency towards complex modeling and deep learning to obtain complex data and transform this data into useful information (Akay and Hess, 2019).

According to the results obtained from the studies on deep learning, it has been suggested that the performance of deep learning in tasks such as visual recognition and auditory recognition is better than people. With this method, medical imaging applications in medicine and health services have attracted attention. Deep learning methods have achieved promising results in medical image analysis (Lee et al., 2017).

The field of radiology is data-oriented. It is convenient to use data processing techniques in this area. Deep learning method has created useful information for image processing in the field of radiology. In addition, it provides accurate diagnosis in the field of radiology, automates tasks and increases efficiency (McBee et al., 2018).

CNNs are used in image processing, they have also shown high success in image segmentation, classification and object detection. CNNs have shown good success in separating complex nonlinear features from images. Thanks to these properties, it is widely used in jobs such as kidney segmentation (Cui et al., 2020).

Vasanthselvakumar et al. (2020) proposed the classification and detection of kidney diseases with deep networks. They used deep CNN to recognize these diseases. In addition, the TensorFlow batch estimation method is calculated to recognize the categories of diseases. They achieved 89.79% performance accuracy for detecting kidney disease. Chronic Kidney diseases 86.67% accuracy rate was achieved by classifying with CNN

According to Onthoni et al. (2020), total kidney volume is required to analyze kidney function losses. The radiologists should use various methods such as measuring the total

kidney volume with medical imaging and dividing the kidney into sections. These processes are time-consuming and demanding. Researchers aimed to design the automatic positioning model of kidney diseases in which the total loss of kidney function should be analyzed using artificial intelligence methods. They designed the image preprocessing and single-shot detector Inception V2 deep learning model using contrast CT images. Researchers have shown that this model achieves better success than other deep learning models in terms of average sensitivity. They explained that this study can help radiologists in the classification and localization of diseased kidneys to improve the calculation of kidney volume.

According to the study presented by Ma et al. (2020), machine learning techniques have an important position due to their high accuracy capabilities for the medical diagnosis of chronic kidney disease whose prevalence is increasing every year. In this study, the researchers proposed a Heterogeneous Modified Artificial Neural Network based on deep learning for early detection and segmentation for chronic kidney failure. This algorithm has the ability to segment the kidney area imaged by ultrasound. In addition, in this study, it was shown that noise was reduced with this proposed method and contributed to the segmentation of the kidney image with high accuracy for determining the location of kidney stones.

Graham-Knight et al. (2019) developed a model for the segmentation of kidneys in CT scans. This model was trained with the KiTS19 data set. The U-Net algorithm has been used and this algorithm can be used to segment images of scans such as CT and MRI. The model has been trained with nnU-Net. It has been defended that this model helps diagnose and treat kidney stones with deep learning. Researchers then applied this model to CT images of patients undergoing kidney stone treatment and achieved overall success. The researchers think that this model needs to be further developed and more research into deep learning tools that help urologists manage the disease process.

Långkvist et al. (2018) developed a computer-aided diagnostic (CAD) algorithm to detect ureteral stones in CT scans. It is aimed to determine non-stone structures and CT volumes with stone density by a CAD algorithm. In this study, CT volume is classified using convolutional neural networks that are successful in computer vision tasks. With this proposed approach, researchers have approached the automatic detection of ureteral stones in CT scans using CNNs.

Ebrahimi and Mariano (2015) worked to provide technical support in the detection of kidney stones. In this study, a semiautomatic program was developed and the effects of the program on image processing, segmentation of the kidney area, and improvement of kidney stone detection were also studied. Researchers have focused on increasing the detection of kidney stones with analysis such as image segmentation and localization, object detection, along image processing techniques. According to the results of the study, they found that the program was capable of imaging small-sized kidney stones that doctors might overlook.

Kolachalama et al. (2018) used DL architecture for chronic kidney disease to better associate biopsy-obtained histological images with clinical phenotypes. The Inception-V3 model, a pre-trained CNN model, was used to correlate these images. This model has been retrained using training classes adjusted for the relevant problem. This deep neural network has been trained using back-propagation and transfer learning is used. In this study, the effectiveness of using deep learning architectures was examined and the performance of a CNN trained on images was compared with a nephrologist. Researchers have stated in the results of the study that this method has different beneficial potential for nephrologists, although it is effective in the clinical decision-making process. They also stated that it is an adaptable method to pathological and histological data sets specific to different organs.

Black et al. (2020) evaluated the use of DL to detect the composition of kidney stones. In a stone laboratory with different types of kidney stones, stones were imaged using a digital camera. ResNet-101 model, which is a deep CNN, is applied to each image. This study is based on the extraction of beneficial properties by classifying the stone compositions and images of CNNs. In addition, with this study, the researchers concluded that stone compositions can be made using DL algorithms.

Parakh et al. (2019) developed a CNN model to detect stones in the urinary system with high performance in non-contrast CT scans with a cascading DL architecture. The researchers chose the Inception-V3 model, a CNN pre-trained with ImageNet, for urinary stone detection because it exhibits high classification performance. This model is then trained with GrayNet and can be used for urinary tract identification and stone detection. They developed a cascading model consisting of two CNNs for the detection of urinary stones. CT sections were defined with these CNNs, and then classifications were made for stone detection. In

the results of the study, it was mentioned that the stepped CNN model can detect urinary tract stones with high accuracy in CT images.

Akshaya et al. (2020) used Back Propagation Network, the algorithm used in the training of neural networks, to detect kidney stones in MR images in this study. Decision-making was carried out by feature extraction and image classification. In this study, feature extraction has been done with principal component analysis and image classification has been done with back propagation network. It has been stated that the back propagation network gives a precise classification compared to other neural networks. With the method used in this study, the location of even small stones in the kidney was determined and the areas with stones could be accurately separated from the image.

Kuo et al. (2019) used DL approaches to automatically determine chronic kidney disease and the estimated glomerular filtration rate after USG of the kidneys. In the neural network architectures of their work, they used the ResNet model integrated with transfer learning. In this study, data magnification schemes were used to extract more features from ultrasound images, and boot clustering was used to prevent over compatibility. This model developed by the researchers is the first step towards improving some of the potentials of ultrasound imaging of the kidneys.

Sharma et al. (2017) used deep learning to examine autosomal dominant polycystic kidney disease, which is a common hereditary disease of kidney disease. It has been suggested to use an automatic segmentation method based on the CNN architecture, VGG-16, to calculate the total kidney volume from computed tomography scans of patients suffering from this disease. It was mentioned that this method by the investigators can facilitate rapid and repetitive measurements of kidney volumes compatible with manual segmentations by clinicians and can be used at a total kidney volume of >500 and $<10,000$ mL.

Manual drawing of the volume of interest (VOI) for the renal parenchyma in CT scans is a long and laborious task. Park et al. (2019) aimed to develop a fully automated glomerular filtration rate quantification method based on a deep learning algorithm for segmentation of the renal parenchyma in CT scans. The deep learning method used is the 3D U-Net network, which is a CNN model. They used CT images and manual VOIs to train this network. According to the results of this study, the researchers showed that the deep learning method

is accurate for renal parenchyma segmentation in CT scans and is successful for automatic measurement of GFR.

CHAPTER 3

CLINICAL BACKGROUND

3.1 Kidney

Kidneys in the human body resemble two bean shapes. These are organs weighing an average of 300g. They are located in the cavity behind the peritoneum. Kidneys constitute almost 0.4% of the human body weight. The kidneys have unique cells and have a different and complex anatomical structure (Briggs et al., 2009; Preuss, 1993). Figure 2.1 represents the human kidney, sectioned vertically (Tanner, 2009).

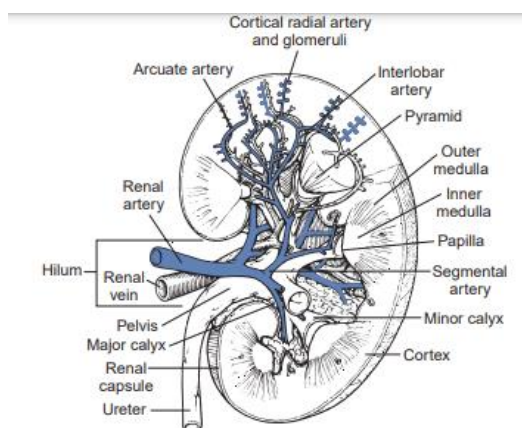


Figure 3.1: The Human Kidney

The position of the kidneys in the body is slightly different from each other, usually, the left kidney is above the right kidney. These are embedded in fat and tissue and kidneys are partially protected by the lower part of the ribs (Preuss, 1993).

The kidneys take on some of the functions in the body. Among them are the functions of maintaining acid-base balance and filtering waste materials in the blood. After such functions, urine formation occurs (Kaur and Juneja, 2018). The unit that performs the functions of the kidney is the nephron. Each adult human kidney contains about 1 million nephrons. Nephrons structurally contain glomerulus and a long tubule, they are composed

of a single epithelial cell. Glomerulus forms the basis of nephrons. The nephrons are subdivided into distinctive parts, they are proximal and distal tubules, the Henle loop, and the collecting channel (Nickolas and Moe, 2019; Briggs et al., 2009). Glomerulars perform the blood filtering function. According to the performance of this function, kidney function is evaluated. For these evaluations, calculations are used that show the amount of filtered blood, named the glomerular filtration rate (GFR) (Nickolas and Moe, 2019; Tanner, 2009). With the functions of the kidney, such as excretion from peritubular capillary blood to tubular liquid, filtration blood through the glomerulus to form plasma ultrafiltrate passing into the bowmans space and re-absorption from the tubular fluid to the blood along the cells-covering the nephritic tubule, unwanted substances are removed and a stable environment is created (Shirley and Unwin, 2010).

The volume and composition of extracellular fluid (ECF) must routinely be regulated. This function is performed by the kidneys. With daily eating and drinking activities, waste and foreign compounds, including beneficial substances taken into the body in large quantities, are removed from the body as urine and the internal environment is stabilized. Osmotic pressure is regulated by removing the urine created from the body. Acid-base balance is achieved and ammonia is synthesized for this. ECF volume and arterial blood pressure are regulated by synthesizing substances that provide Na^+ excretion. The ion density of the blood plasma is adjusted. They make the polypeptide hormones break down. Among the waste products of metabolism are urea, creatinine, and uric acid. The kidneys remove these waste materials. Substances that provide renal blood flow and hormones such as vitamin D3 and erythropoietin are produced in the kidneys (Tanner, 2009).

In arrange for the blood plasma to be highly filtered, there must be high blood flow in the kidneys. There are many factors that affect the blood flow rate. These may be local hormones and intrinsic factors such as autoregulation. In addition, there may be external factors such as blood-borne hormones and nerves (Tanner, 2009). The kidney's functions include regulation of blood pressure, red cell count, and bone density (Little and Combes, 2019).

As a result of the various daily activities of people, changes occur in the volume and composition of the fluids in their bodies. The kidneys function to bring these changes to normal values. In healthy kidneys, these functions are performed in a short time and then ion

concentrations do not deteriorate for a long time. On the other hand, deviations in these functions occur in unhealthy kidneys or in some disease states thus normal values in the composition and volume of body fluids deteriorate (Briggs et al., 2009). Based on data from the World Health Organization (WHO), problems in kidney function are a global illness. In case of early diagnosis and treatment, the increase in kidney function disorders can be controlled (Kaur and Juneja, 2018).

3.2 Kidney Stone

Kidney stone, known as a urological disease, is crystal solidification that occurs in some parts of the kidney. It is known that kidney disease affecting human health in the world population affects 12% of the population. Urinary system stones date back to many years BC. People have suffered from kidney stones, a common urinary tract disease, for a long time (Alealign and Petros, 2018). For many years, the urinary tract stone disease was known as the human problem. However, in recent years, the form of the disease and the oftenness of stone formation have changed beyond negligence. In the past, stone formations were frequently seen in the bladder. But, nowadays, upper urinary tract stones are often seen (Fig. 2.2) (Espinosa and Esposito, 2020).

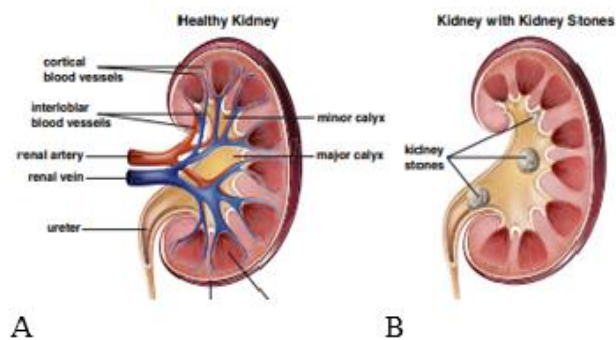


Figure 3.2: (A) Healthy Kidney, (B) Kidney with Kidney Stones

The researchers put forward a study to compare glomerular filtration rates. In this proposed study, data from the National Health and Nutrition Examination Questionnaire III were used, and people with kidney stones and those with a BMI of 27 or above were selected. According to the results, these individuals were found to have a lower glomerular filtration rate (GFR) than those without stones. In terms of blood pressure, it is known that people with stones have a higher blood pressure than people without stones. It is known that the kidneys of patients suffering from kidney stone disease are damaged during the stone formation process, their kidney functions decrease, and their blood pressure increases (Coe et al. 2005). Stone formation in the renal tubules or collecting system can be called nephrolithiasis and nephrolithiasis has significant morbidity (Monk and Bushinsky, 2010).

Kidney stones can remain asymptomatic for many years. Until the stones require medical attention, it is generally not known when the stone begins to form. It can be understood whether there are stone-forming factors by looking at the life routine of the patient. The recurrence rate of the disease can be predicted, but definitive results are obtained with imaging studies (Curhan, 2014).

3.2.1 Epidemiology

When nephrolithiasis is examined globally, it is seen that the prevalence and recurrence rates of this disease have increased (Alelign and Petros, 2018). When kidney stone formation was compared by gender, it was observed that there was a 3: 1 ratio in stone formation in men. However, when looking at the incidence of nephrolithiasis, it is seen that it increases in women and decreases in men, and the incidence of kidney stones tends to gender equality (Espinosa and Esposito, 2020).

According to epidemiological studies, in the last decade, when diagnosing nephrolithiasis, an increase in the incidence of kidney stones has been observed for all age groups (Edvarddon et al., 2013). According to some criteria, there are differences regarding the occurrence of kidney stone disease. These can be listed as gender, age, genetics, geography, climate, diet, fluid intake, occupation (Sorokin et al., 2017). For example, while calcium-based stone types are seen in the United States of America; uric acid originated stones are

seen in the Mediterranean and the Middle East. In other words, differences can be seen in stone types according to geography and genetic predisposition (Monk and Bushinsky, 2010).

3.2.2 Kidney stone creation

Biomineralization or stone pathogenesis occurring in the kidney is a very complex formation process. Solvents precipitated in the urine cause nucleation due to the excessive saturation of the urine and as a result of this, crystallizations are formed. Crystallization is induced by supersaturation, and this is called the upper metastability limit, and this is a process required for kidney stone formation. In short, the over-saturation of urine and physicochemical changes in the kidney represents a biological process in stone formation. It is necessary to investigate the causes of nephrolithiasis to regulate the treatment of kidney stones and reduce the frequency of future cases (Alelign and Petros, 2018; Pfau and Knauf, 2016).

3.2.3 Sites of stone growth

According to researches, calcium phosphate compounds form deposits on the tip of the kidney papillae. These are known as the main reason why calcium oxalate stones are formed. This area has been developed with some researches; Plaque forms at the base of the thin folds of the Henle and moves along the tissue, in the renal tubules, and around the vasa recta. Finally, it protrudes into the uroepithelium in the kidney papillae. It is important to choose the appropriate treatment for people with kidney stone disease. Plaque formation mechanisms must be well understood in order to determine the appropriate treatment correctly (Pfau and Knauf, 2016).

Kidney stones are classified according to the location of the stones. Stones that fill the pelvis and extend into the calyces are called non-staghorn or either staghorn. Those located in the distal and proximal positions are called ureteral stones (Evan, 2010). Different stone compositions can be seen in different and complex structures according to their formation. Asymptomatic stones are usually growing in the kidney calyces (Brisbane et al., 2016),

3.2.4 Stone types

The structure and chemical content of kidney stones change according to the deterioration in the composition of different chemicals found in urine. In other words, the shapes and sizes of kidney stones depend on different chemical compositions found in urine. Kidney stones variation widely according to their formations and compositions. These stone types;

1. Calcium phosphate and calcium oxate based, calcium stones
2. Struvite (triple phosphate)
3. Uric Acid or Urate Stone
4. Cystine Stones
5. Drug-Induced Stones

(Alealign and Petros, 2018).

Kidney stones can also be categorized as non-calcerius stones, radio-opaque stones, and calcium-based stones. There are cystine stones among the stones that are radio-opaque because cystine stones contain sulfur in them. Radio-lucent stones are indinavir stones and uric acid stones (Parmar, 2004). The composition of many of the crystals occurring in the kidneys is of calcium origin, complicated with phosphate and oxalate. Combinations of non-calcium stones usually consist of struvite stones, cystine stones or uric acid stones that are formed in combination or (Briggs et al., 2009)

The size of the stones in the kidneys differs. If the stone size is 7 mm or more, urological intervention is usually required for this stone. If the stone is 5-7 mm in size, the chance of passing through the urinary tract is 50%. Stones smaller than 5 mm can usually pass through the urinary tract. 90% of the stones in the kidneys can pass through the urinary tract, but surgical intervention is required for other stones. These interventions include stone fragmentation by the non-invasive shock wave lithotripsy, ureteroscopy, or removal of stones by percutaneous nephrolithotomy (Evan, 2010).

Stone analysis is of great importance when evaluating the mechanisms of stone formation. In the diagnosis and treatment process of patients with kidney stones, useful information can be obtained through stone composition analysis (Briggs et al., 2009).

3.2.5 Risk factors for kidney stone creation

Urine compositions can vary depending on a person's diet and medications. Nephrolithiasis occurs due to abnormalities in their chemical composition in the urine. For this reason, urine may cause an increase in the incidence of kidney stones.

1. A person's daily fluid intake affects their urine composition. Low fluid intake leads to increased urine concentration and increases the likelihood of nephrolithiasis. People which are living in hot climates have an increased risk of composing kidney stones.
2. Some drugs change the pH of the urine and may cause crystallization, therefore stone formation may occur.
3. Plenty of consumption animal's foods creates oxalate excretion and lowers urine pH. For this reason, uric acid stones may occur.
4. High amount of urinary oxalate excretion is a risk factor for the formation of kidney stones.
5. Consuming foods containing high amounts of potassium can reduce the risk of developing kidney stones.
6. Consuming foods rich in calcium are associated with nephrolithiasis.
(Pfau and Knauf, 2016).

Several other non-dietary risk factors exist:

1. Nephrolithiasis has a genetic predisposition. In other words, if a person has kidney stones in his family, his risk increases 2.5 times.
2. Some diseases can increase the risk of kidney stone formation. These diseases include Crohn's disease, renal tubular acidosis, and hyperparathyroidism.
3. Gout increases the risk of nephrolithiasis.
(Mayans, 2019).

There are many treatments for kidney stones. These treatments are; drug therapy, extracorporeal shock wave lithotripsy, conservative therapy, ureteroscopy, and invasive surgical stone removal. The most appropriate treatment for a patient with kidney stones is determined according to the size and location of the stone, and different treatments are used for each patient (Reimer et al., 2020). Before the treatment is decided for a kidney stone

patient, the complex anatomy of the kidney, areas without stones in the kidney, the duration of the surgery, and the amount of blood loss should be evaluated. The information obtained from these evaluations is useful for the urologist regarding optimal treatment. The most important information for a patient's kidney stone is obtained by imaging the kidney (Motamedinia et al., 2015).

3.3 Kidney Stone Imaging

Kidney stone imaging is preferred for the diagnosis and treatment planning of nephrolithiasis using different imaging methods. Kidney imaging is also very important for disease follow-up after optimal treatment or surgical interventions (McCarthy et al., 2016). It is aimed to determine the position of the stone by imaging the anatomy of the kidney such as renal pelvic and calyceal with imaging methods. Imaging is used to determine whether the kidney functions are fulfilled, at the same time to choose the correct treatment method for patients with kidney stones and to understand whether the treatment is successful (Rao, 2004).

Imaging has been the most effective method for the urologist to diagnose patients admitted to the hospital with some complaints about the kidneys. It also helps in determining the location and size of kidney stones after diagnosis, which is the first step. There are many different imaging methods to image the nephrolithiasis. The most appropriate method should be selected by considering factors such as cost, ionizing radiation and the body structure of the person to be imaged (Brisbane et al., 2016). Imaging modalities allow choosing the optimal method for kidney stones from treatment modalities such as shock wave lithotripsy (SWL), ureteroscopy, or percutaneous nephrolithotomy (PCNL) (Dhar and Denstedt, 2009).

Imaging methods used to imaging the kidneys and diagnose kidney stones include computed tomography (CT), ultrasonography (USG), kidney, ureter, bladder plain film (KUB), magnetic resonance imaging (MRI), and intravenous urography (IVU). When looks at the use of imaging methods in the past, we see that intravenous urography has been used frequently, but then this method has been replaced by CT. There are advantages and disadvantages to each of the imaging methods. Different methods can be chosen according to variable and special situations (Mayans, 2019).

3.3.1 Noncontrast computed tomography

CT is a method that can perform image scans with and without contrast, with different image timing according to different clinical situations (Brisbane et al., 2016). Computed tomography has imaging capability with good spatial resolution and high contrast. Through these features, they can enable urologists to detect abnormalities in the kidneys by imaging the kidneys on CT. They create non-invasive cross-sectional images of the target organ for the diagnosis of many diseases, including nephrolithiasis. (Kaur and Juneja, 2018).

The first step to make a diagnosis is high-resolution imaging of the abdomen and pelvis area. Unenhanced computed tomography is used for this. Through to these images, nephrolithiasis can be evaluated. It has been reported that the success rate of CT imaging technique in the diagnosis of kidney stones is 95% (McCarthy et al., 2016).

Contrast material is not used when imaging kidney stones because the structures of different composition of kidney stones absorb radiation at a high rate. In this way, images are evaluated easily. In Figure 2.3, an occlusive stone appeared in the left image, a non-occlusive stone appeared in the right image. (Brisbane et al., 2016).

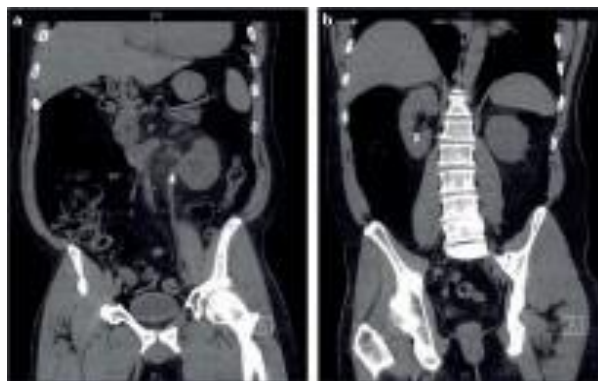


Figure 3.3: Imaging of kidney stone with non-contrast CT

Axial sections obtained without the use of contrast with CT are imaged from the upper part of the kidneys to the pelvis position. These images are evaluated together with sagittal and

coronal reformats. Calcium-based kidney stones can be well visualized with non-contrast CT. However, uric acid stones, which are radiolucent on plain radiography, are successfully imaging on CT (McCarthy et al., 2016).

CT imaging method detects the stone in the kidneys and at the same time allows it to be detected in other abnormalities in the urinary system by imaging from the upper part of the kidney to the lower part of the bladder in the area of view (Eisner et al., 2011). Reliable imaging of factors such as stone location and stone size is very significant for the correct management of kidney stone diseases. Figure 2.4 shows stone detected in the collecting system of the patient left kidney (McCarthy et al., 2016).

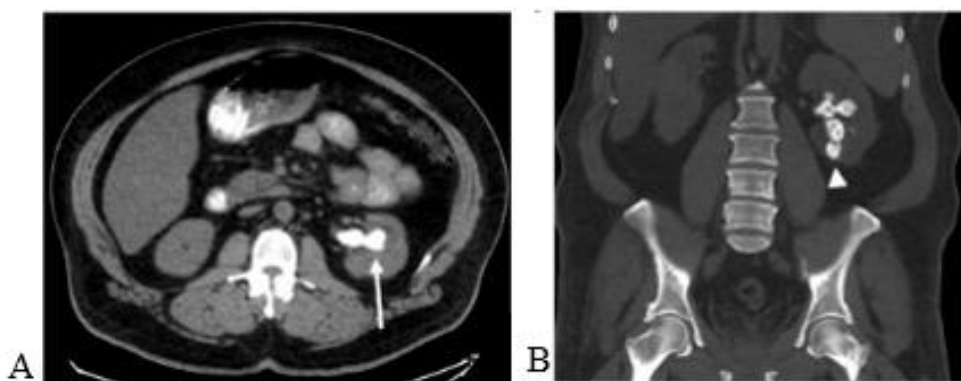


Figure 3.4: (A) Axial and (B) Coronal non-contrast CT images

Photons are exiting the X-ray tube reach the detector after the object it encounters. The attenuation values of the photons coming to the detector show the density of the object. These attenuation values are the Hounsfield unit (HU) measure. According to the HU measurements, the value of water is 0, the value of bone is 1000 and the value of air is -1000. Kidney stones absorb different amounts of radiation according to stone composition. Stone compositions can be determined by looking at their radiation absorption values. With Ct imaging, the HU value of uric acid stones is between 200- 400, and calcium oxalate stones have a HU value in the range of approximately 600-1,200 (Brisbane et al., 2016).

It is important to distinguish between kidney stone types structurally. For example, through to Ct imaging, uric acid-based stones and non-uric acid-based stones can be distinguished

and disease management can be made more accurate. The researchers showed that with their HU values, they could easily distinguish uric acid stones from other stones. It is very important to know the stone density for the treatment of shock wave lithotripsy (SWL). The HU density of the stones enabled SWL to be successful (Eisner et al., 2011).

CT can image two-dimensional stone area and three-dimensional stone volume. If these images are evaluated correctly, the success rate of extracorporeal SWL used in the treatment of kidney stones increases. Determining the volume of the stone is important for complex stone compositions. For example, the either staghorn stone has a complex structure and the volume of the stone must be known in order to determine the stone load correctly (McCarthy et al., 2016). CT attenuation values are used to evaluate whether SWL therapy is effective or not. If the attenuation increases, the number of shocks required increases and the success rate decreases. Also, voxel on a stone can decrease the HU values. This may cause a stone to be less dense and cause a misinterpretation of SWL. This problem can be solved by using dual energy CT. The dual-energy CT method displays at two voltages and allows comparison of data from two detectors. In this method, different energies can be used according to the target area. It is useful for tissue assessment and also enables a more accurate assessment of stone compositions (Brisbane et al., 2016).

CT is an ideal method for imaging kidney stones and its use is increasing for this. However, the use of ionizing radiation is a concern for young patients, pregnant women, recurrent kidney stones and patients vulnerable to radiation (Ibrahim et al., 2016). In such special cases, radiation exposure poses a serious problem. Researchers have been working on reducing the radiation dose used in CT. Low-dose CT has also been found to exhibit comparable sensitivity and specificity (Mayans, 2019).

By reducing the tube current to the radiation source, radiation exposure can be reduced for low-dose CT. 100 Ma tube current is used in often used CT without contrast. In low-dose CT for radiation reduction efforts, this value may decrease up to about 30 Ma and below. With lowering the radiation dose, image accuracy and quality may decrease. Low-dose CT can be used to scanners stones in the kidneys but, the ability to imaging kidney stones smaller than 3 mm becomes difficult. Generally, in different patients, CT settings can be changed according to the patient's body structure and the area to be imaged. In order to make the most

appropriate imaging settings in CT, attention is paid to the patient's age, BMI, and the grade of the suspicious stone. Image data that can be accessed by standard CT can also be accessed using low-dose CT. In scanning for kidney stones, it was seen that both could provide the accurate stone location, size, attenuation data, and stone composition (Brisbane et al., 2016).

The cost factor is a significant disadvantage to CT. The same is true for low-dose CT. CT cost may be reduced or increased compared to other radiology imaging techniques. Cost is a disadvantage that distinguishes CT from ultrasonography. However, it is a very important factor in radiation exposure (Brisbane et al., 2016).

There have been useful studies on CT used in urological diseases. Multiple Detector CT (MDCT) and Dual Energy CT (DECT) technologies have been developed by expanding the scope of CT (Andrabi et al., 2015).

- **Dual energy computed tomography (DECT)**

With the technological development of CT, which has an important role in the imaging of kidney stone disease, DECT is also widely used (McCarthy et al., 2016). Data for imaging the kidneys using DECT is obtained by scanning at two different energies. The structural composition of the scanned object is evaluated by the attenuation data. Can create object-specific images (Ibrahim et al., 2016).

DECT can create a virtual image of the kidney without using contrast. Through the virtual image created, the types of kidney stones can be distinguished. Each kidney stone type has different compositions and attenuation coefficients (Mayans, 2019). The attenuation data from the two energy sets are calculated with a mathematical formula. The software is then used to generate the color-coded map. Figure 2.5 shows kidney stones imaged using DECT (McCarthy et al., 2016).

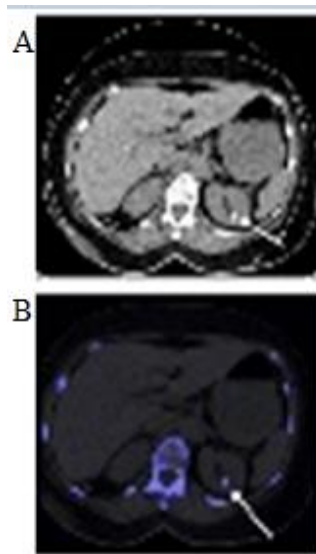


Figure 3.5: (A) Axial Kidney Image, (B) Color-Coded Map Used Image

- **Multi-detector computed tomography (MDCT)**

MDCT was introduced in 1998. MDCT can be used to scanners urological stones. Makes three-dimensional reconstructions of urinary stones and makes multi-planar reformations. In this way, it provides the opportunity to evaluate the position and size of the stones. MDCT makes the volumetric analysis of stones and contributes to the treatment phase by evaluating the attenuation of the stone composition of HU. MDCT has also been shown to improve pre-treatment characterization for the composition of stones. MDCT is being used more than DECT (Andrabi et al., 2015).

3.3.2 Ultrasonography (USG)

Ultrasonography can perform imaging quickly and at a low cost. Provides 2D images of organs and tissues. It performs imaging by non-invasive method and using high-frequency sound waves (Kaur and Juneja, 2018).

An ultrasound is usually used to imaging kidney stones (Rao, 2004). High-frequency waves used in USG cannot pass through kidney stones. Therefore, USG waves reflect strongly and

glare appears in the image. The imaged stones cast shadows. Soft tissues cannot transmit high-frequency waves like stones and cannot reflect strongly (Brisbane et al., 2016).

It is possible to image the anatomical structures and abnormal conditions in the kidneys with USG. Pathogenic conditions can be evaluated with USG images. It is easy to detect large kidney stones that cause acoustic shadowing on USG. However, it becomes difficult to detect stones smaller than 5 mm in US imaging. Figure 2.6 shows an ultrasound image of a patient kidney with a history of nephrolithiasis (McCarthy et al., 2016).



Figure 3.6: A stone was identified with the sagittal view of the left kidney

There is no harm in repeating the patient imaging with ultrasound because it does not contain radiation and there are no other side effects. Stones in the kidney are imaged quickly and at a low cost. Radiolucent stones can be detected by USG. Since it is good at finding stones in ESWL treatment, imaging can be performed during treatment (Rao, 2004).

There are more USG devices than CT scanners in the world (Mayans, 2019). Although USG provides imaging for the diagnosis of kidney stones, it is also the optimal imaging option for patients with special conditions. For example, it is very beneficial for the urologist to use USG in pregnant women, young patients, and people with sensitivity to ionizing radiation (McCarthy et al., 2016).

USG has such advantages but has some limitations as well. USG is used to track the treatment of existing stones in a patient's kidney. Among the limitations of USG, there is the difficulty of detecting small stones. It is also difficult to image obese patients. Compared

to radiography, ultrasound has less sensitivity in imaging kidney stones (Pahira and Pevzner, 2007). Ultrasound resolution may not be sufficient when imaging small stones. The dimensions of the reflected beam can look like small stones and cause misunderstanding of the stone dimensions. Therefore, the urologist should be careful while evaluating the images obtained with ultrasound (Brisbane et al., 2016).

3.3.3 Kidney ureter bladder radiography (KUB)

KUB is a radiographic method of imaging in a single plane. In this method, a single source of light is required to produce photons. The produced photon passes through the tissue oriented anterior to posterior and encounters the contralateral receiver (Brisbane et al., 2016). KUB plain film radiography has easy use. The rate of exposure to radiation is low. Its utility in detecting radiolucent stones is limited, but imaging of medium-sized radio-opaque stones is successful. However, as the stone decreases in size and stone-like structures such as shadows of calcified mesenpheric nodes, it is difficult to distinguish (Rao, 2004).

The KUB method can image the target organ or tissue from a single angle. Since it is imaging the kidneys from a single angle, the values of specificity, sensitivity and accuracy decrease and therefore its benefit of this method is also reduced. Kidney stones can be imaged using this radiography method, but not all. For example, it does not have the ability to visualize martix and uric acid stones but, struvite and cystine stones can be imaging at a low degree. The KUB method is considered to have a specificity of 76% and a sensitivity of 57% (Brisbane et al., 2016). The KUB method is not as sensitive as other imaging methods, but it can provide valuable information for ureteroscopy, shock wave lithotripsy and percutaneous nephrolithotomy, which are kidney stone treatment methods (Eisner et al., 2011).

KUB method, like other imaging methods, has benefits and limitations. KUB limitations include the inability to view stones smaller than 2 mm and non-opaque stones. In addition, it is difficult to distinguish a supine scanned kidney from extrarenal calcification. The advantages of this method include its speed, low cost, and easily imaging (Pahira and Pevzner, 2007). Another advantage is that it contains a low dose of radiation. But, the

physical body structure and intestinal gas of the person who will be screened with this method are factors that can limit the success of imaging (Dhar and Denstedt, 2009).

3.3.4 Magnetic resonance imaging (MRI)

MRI is performed according to the principle of aligning the protons of the patient to be imaged to the magnetic field axis using a magnetic field (Brisbane et al., 2016). Radiation is not used in MRI. Imaging of kidney stones can be performed with this method. But, kidney stones may be indistinguishable from other tissues and may be confused with artifacts. Because the echo times (TEs) used for imaging are not short and the magnetic resonance signals from the stones decrease very quickly (Ibrahim et al., 2016).

The MRI method cannot create a direct visual of kidney stones, it relies on cavities and calcifications. It is not preferred for most cases because the imaging time is long and the cost is high. However, since it does not contain radiation, it is used as an alternative option in pregnant patients who cannot obtain successful imaging with ultrasound (Mayans, 2019).

When CT and MRI method are compared, it is seen that MRI is three times more costly than CT. It also has less accuracy and longer imaging time. The magnetic resonance imaging method appears to have a low success rate compared to computed tomography, for imaging kidney stones. With develops in technology, there is a need for ultra-short echo time sequences of MRI. Because to measure stone size more accurately, must increase sensitivity and specificity values (Brisbane et al., 2016; Rao, 2004).

3.3.5 Intravenous urography (IVU)

Serial radiographs are obtained with an intravenous urogram. It is based on the method of imaging the renal tract by injecting iodine-containing contrast material into the body of the patient to be imaged with IVU (Kaur and Juneja, 2018). In order to perform imaging, the KUB is first made and then iodinated contrast material is injected intravenously. Then, sequential images of the kidneys are created within 30 to 60 seconds. The shape and size of the kidneys are evaluated with the nephrogram. In order to view the anatomical structure of the calyces, the pelvis can be imaged within 5 to 10 minutes (Clarkson et al., 2010).

Historically, intravenous urogram was the visualization method chosen as the optimal standard for treatment planning for urinary system stones. In this method, radio-opaque contrast material is used and this contrast material is sent to the collecting system of the kidney and thrown into glomerular filtration. In this way, the anatomical structures of the renal pelvis, ureters, and calyces are successfully imaging (Dhar and Denstedt, 2009). Nowadays, it is said that the IVU method is no longer used to view kidney stones. Because non-ionic contrast agent injection is done and this can cause an allergic reaction in patients. In addition, serious problems may occur if metformin is given while using this method for patients with metabolic disorders. It contains high radiation. It has a long imaging time and gives poor anatomical data about the imaging area (Rao, 2004).

The IVU method allows the visualization of obstructions in the kidney ducts. However, since contrast material is used, the use of this method in allergic patients is inconvenient. At the same time, it is inconvenient to use in pregnant women and young patients. Because it contains more radiation dose than plain radiographs (Kaur and Juneja, 2018). As long as a sufficient degree of imaging is obtained, ultrasound or plain radiography methods of the abdomen can be used for imaging. Because during the treatment of diseases, harmful radiation is avoided (McCarthy et al., 2016).

If CT, MRI, USG, and KUB methods, which are the methods used to image kidney stones, are improved with technological developments, the possibility of correct imaging of kidney stones may increase (Brisbane et al., 2016). In conjunction with these imaging methods, improvements can be made for imaging if DL is used. Convolutional neural networks are used for image processing, image classification, and image segmentation because CNN's perform well for them. CNN's also perform image segmentation in complex structures such as kidneys. Thus, it can extract nonlinear features from complex images (Cui et al., 2020).

CHAPTER 4

CNN'S APPLICATION IN KIDNEY STONE ANALYSIS

This section provides detailed technical background on deep learning algorithms. CNN, which is the main deep learning method, and 5 different CNN architectures chosen to apply to CT data in which kidney stones are imaged were introduced in technical details. Finally, this section presents the application of selected 5 CNN architectures to CT images of the acquired kidney stones.

4.1 Deep Learning

Deep learning (DL) is a new development with some improvements. Deep learning is a method for improving the performance of Machine Learning (ML) tasks (Erickson et al., 2018). Deep learning is an improved type of artificial neural network (ANN) that is part of ML. ANN was introduced in 1950, however, it has some limitations. These are problems that hinder the training of gradient and deep architecture and cause deficiencies such as computing power. Also, there are serious limitations such as overfitting issues to solve real dilemmas. Many new developments have been made to resolve these limitations. These are new algorithms for training graphics processing units (GPUs) and deep neural networks (DNN) to use big data (Lee et al., 2017).

The task of the first layer of DNN networks, which consists of many layers, is to make predictions for observed values. The first layers where these predictions are made are named the input layers. The layer where a value is produced or a class is estimated is called the output layer. There are also hidden layers in the architecture. These are located between the first layer, the input layer, and the last layer, the output layer. Thanks to the layered structure, it enables neural networks to make decisions for more complex structures with combinations. Figure 4.1 shows a representation of deep learning neural networks and artificial neural networks (Lee et al., 2017).

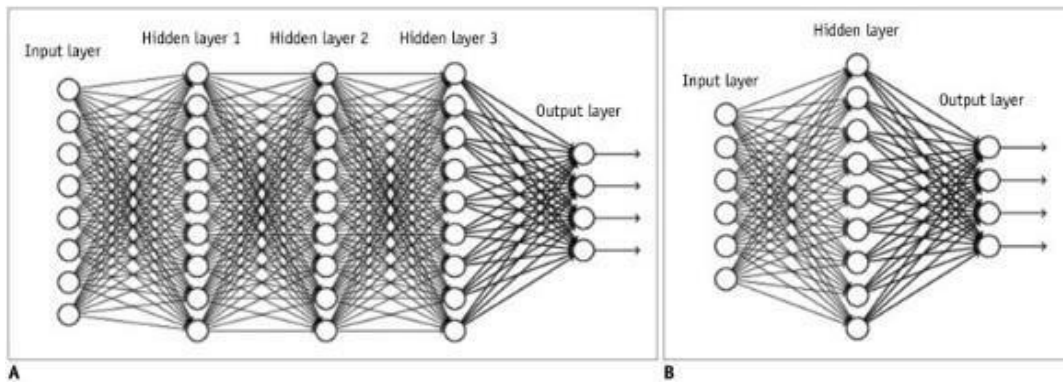


Figure 4.1: (A) Deep Learning Neural Network, (B) Artificial Neural Network

DNN consists of deeper layers than ANN. Therefore, it has a more complex layer structure. Through to the complex layers, DNN's ability to predict and recognize is further improved (Lee et al., 2017).

The work of Krizhevsky and colleagues make a crucial contribution to the transformation of machine learning into deep learning. With the deep learning model called AlexNet in Imagenet 2012, the researchers found a classification error of 15.2% by classifying 1.2 million high-resolution images in 1000 different classes. The first deep learning model in ImageNet is AlexNet, a five-layer convolutional neural network. The error value, which was 15.2% when it was first introduced, was then reduced to 2.25 (Saba et al., 2019).

Multi-layer computing models are used in DL compared to machine learning. For example, in the segmentation of organs or disease classification, high-level representation of complex data is learned by means of the multi-layered structure. In DL, features are automatically learned over the noisy and raw data of the algorithms compared to ANN. However, radiological feature extraction and pre-processing are required in ANN. Therefore, DL has superior education and learning ability compared to ANN. DL gains this capability by using its nonlinearity and dimensionality reduction features (Saba et al., 2019).

By means of the developments in deep learning methodologies, the speed of information processing has also improved significantly. The advancement of computing speed has come with the availability of GPUs in DL calculations. DL algorithms using the GPU run much faster compared to central processing units (CPUs). Because GPUs have the ability to do

many calculations and thousands of processing units at the same time. DL algorithms using GPUs work much faster than CPUs. Also, an important factor for DL is the rapid increase of GPU card memory (Erickson et al., 2018). Computing time for complex transactions is shortened with DNN training. This was made possible by the development of the GPUs information processing unit. In this way, large amounts of unclassified data are analyzed by DL and then the model is trained to predict accurately, then produces meaningful and powerful results (Lee et al., 2017).

4.2 Convolutional Neural Network

Among deep learning methodologies, convolutional neural networks (CNNs) have a very important place for image analysis (Altaf et al., 2019). There are many deep neural network models. However, CNNs are the most used. There are mathematical linear operations between matrices called convolution, and this is where the CNN is named (Albawi et al., 2017). The connection structure of neurons in the visual cortex of animals has been a source of inspiration for CNN, when successfully trained, can generate hierarchical information. It can generate hierarchical information during classification, for example, when preprocessing such as edge, shape determination and object structure determination (Lee et al., 2017).

Computer vision area is an upper domain of CNNs. CNNs have been used in this area for many years. However, after the ImageNet Large-Scale Visual Recognition Challenge (ILSVRC), CNNs great success became increasingly understood. Its success is due to the efficient use of GPUs in this model, its effective data enhancement feature, its ability to provide corrected linear units, and the new dropout arrangement. CNN has become a successful model thanks to its deep architecture. Because, with its deep architecture, it has the ability to extract distinctive features at multiple levels of abstraction (Taibakhsh et al., 2016).

CNN has different layers in its architecture. These layers contain weights, and the image can be classified using these weights and features learned by bias (Roy and Islam 2020). CNN uses minimal processing capability to recognize visual patterns from pixels through its multilayer neural network. CNN can amalgamate the low-level layers with the properties of

the high-level layers that come after it. For example, they can amalgamate low features like lines and edges with higher properties like shapes (Monshi et al., 2020).

A typical CNN; it is a mathematical structure consisting of three layers: convolution, pooling and fully connected layer. The feature extraction task belongs to the convolution and pooling layers. The process of classifying the extracted features takes place in a fully connected layer (Yamashita et al., 2018). CNNs must have the input layer format suitable for the input data. It should also have the identical output layer form as the teaching data. When doing multiple classifications, units in the output layer of the network used must be equal to the number of categories of teaching data. The layers between the input layer and the output layer are called hidden layers (Yasaka et al., 2018).

There are stages for the training process to take place in CNN. First, layer-by-layer operations are carry out after input data is received by the network. After these operations, it gives a final output to compare the correct result. There is a difference between the produced result and the desired result, and the error is equal to this difference value. This error has to be transferred to all weights in the layers. A back propagation algorithm is used for this transfer process. Weights are updated through iterations to reduce error (Özkan and Ülker 2017).

A typical CNN architecture has several convolution and repetitive pooling and one or more fully connected layers. Figure 4.2 shows the representative CNN architecture (Yamashita et al., 2018).

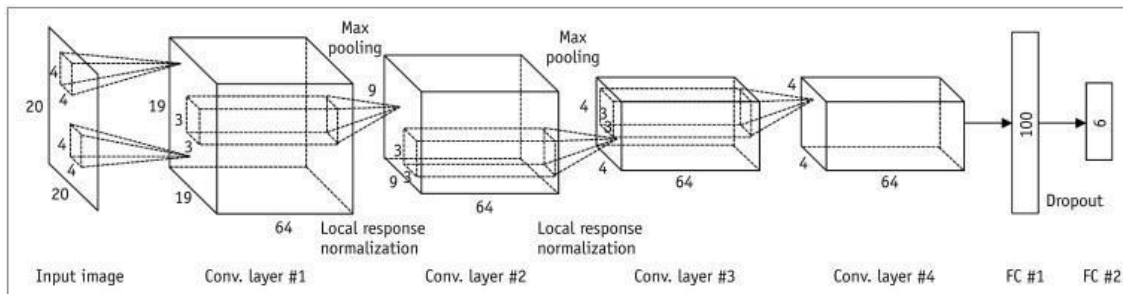


Figure 4.2: Architecture of CNN

There are very few connections between CNN layers. In this way, it can preserve the spatial relationship of the data. The first layers are created with an architecture such as a grid shape. The input layers are then fed from the layers that control these relationships. Layers process in CNN runs on part of the previous layer. Figure 4.3 shows the structure of a typical CNN (Lundervold and Lundervold 2019).

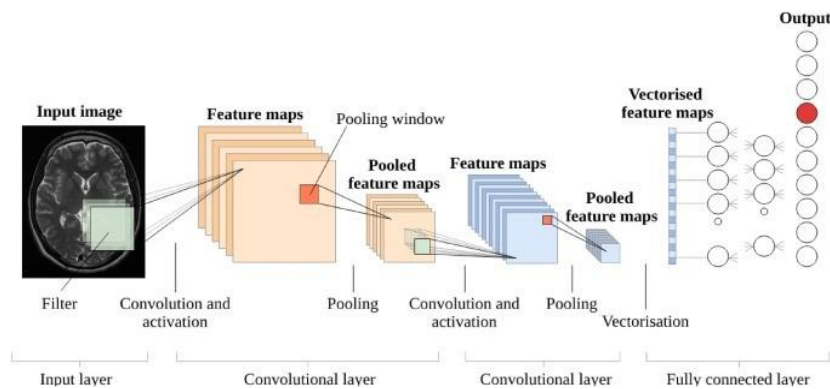


Figure 4.3: Structure of a typical CNN

- **Convolutional Layer**

Convolutional layers have some functions. Among these are detecting certain properties of the input data at all locations. In order to detect this data, the nodes of the convolutional layers must be connecting to a subset of their spatial neurons in the input layers. The task of the convolutional layers is to identify certain properties. For this, the connection weights are shared between the nodes of the input layers. This set of weights is named a core or convolutional core (Taibakhsh et al., 2016).

Convolutional layers aim to detect lines, distinctive edges, and other visual elements. To learn the values of the input layers, which are special filter tools, some processing is required. The purpose of this mathematical operation is to explain to multiply a pixel's local neighbor's kernels. This process learns the meaningful kernels and mimics features such as edges and colours to those introduced for the visual cortex. It may be preferable to use filter banks for these operations. Each of the filters is a square object, and they are moved on image. The image values obtained in this way are collected with filters. Multiple filters are applied on

convolutional layers, resulting in multiple feature maps (Lee et al., 2017). Convolutional filters or kernels perform the convolution process on the image. One of the purposes of convolution layers is to learn the weights of these convolutional filters or kernels. In the past, such filters were used in traditional image analysis methods to highlight and feature different images. For example, the Sobel filter used to detect edges in images. Before CNN methods, the weight of the beans had to be adjusted manually with filters. With the developments in CNN, these settings have been learned automatically (Altaf et al., 2019).

For convolution processes, weight sharing creates some properties. First, the kernels move to all positions of the image and detect learned features, and then feature extraction is allowed to change feature patterns. The second feature of weight sharing is; by learning the hierarchies of feature models together with a pooling process, a wider field of vision is created. Finally, the number of parameters is reduced to increase model efficiency through Weight sharing (Yamashita et al., 2018). The operations performed in convolution layers are important for CNNs. Convolution processes are successful in classification, segmentation, and image processing tasks. Figure 4.4 represents a convolution process (Lee et al., 2017).

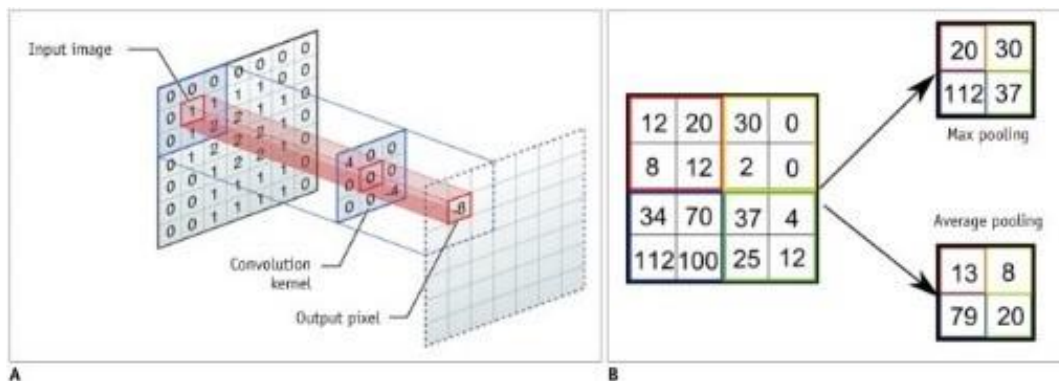


Figure 4.4: Convolution Process

- **Rectified Linear Units Layer (ReLU)**

By virtue of the nonlinear activation functions, feature maps created in the Convolution layer are fed. With this feed, the nearly entire neural network is approximated to the nonlinear

function. Usually rectified linear units are used for activation functions. ReLu is defined as follows; $ReLu(z) = \max(0, z)$ (Lundervold and Lundervold 2019).

Rectified linear units with simpler activation functionality work better for deep learning than sigmoidal functions (Erickson et al., 2018). Sigmoid and tanh nonlinear states were popularly used for many years. However, recently ReLu has been used more frequently. Because, ReLu's both gradient definition and function definition are simpler.

$$ReLu(x) = \max(0, x) \quad (4.1)$$

$$\frac{d}{dx}(x) = \{1 \text{ if } x > 0; \text{ otherwise}\} \quad (4.2)$$

The gradient signal starts to disappear as the network deepens, and this is called the nonbolan gradient. The reason for the disappearing gradient is because the gradient of these functions is close to zero in most places. ReLu has a steady trend. Finally, sigmoid and tanh mostly have non-zero gradient values. This situation may not be suitable for education. A less frequent representation of ReLu is created. Because the zero in the gradient ensures an exact zero (Albawi et al., 2017).

- **Pooling Layer**

Data is fed by many convolution layers. A feature map is created with the feed. It is then pooled in the pool layer between the convolution layers. Pooling uses grid regions as input and produces single numbers for those regions. This is then calculated with the average or maximum pooling function. Due to the shift in the data in the convolution layer, differences in the activation maps may occur and translation invariance occurs in the pooling layer. (Lundervold and Lundervold 2019).

The function known as maximum pooling is a pooling function. This maximum pooling function takes the known maximum input value of the convolutional layer. In this way, the maximum pool layer reduces the memory and resolution requirements for the image by making the best estimate for the sampled region (Erickson et al., 2018). Figure 4.5 represents a maximum pooling process (Doğan and Türkoğlu, 2019).

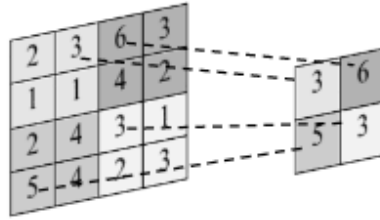


Figure 4.5: Maximum Pooling Process

- **Fully-Connected Layer**

In the CNN structure, after the successive convolution, ReLu and pooling layer comes the fully connected layer. The fully connected layer is bound to all areas of the layers that precede it. Different network structures can have a different number of layers. (Özkan and Ülker 2017).

In CNNs, the dimensions of the activation maps is gradually reduced. This reduction function is performed using convolutional and pooling layers. Next, the activation maps from the deeper layer are rearranged in fully connected layers (Altaf et al., 2019). In the CNN structure, the properties are learned in the layers located before the fully connected layer. Then these features combined in this final layer, the fully connected layer, to decide (Erickson et al., 2018). Figure 4.6 shows a representation of the fully connected layer (Doğan and Türkoğlu, 2019).

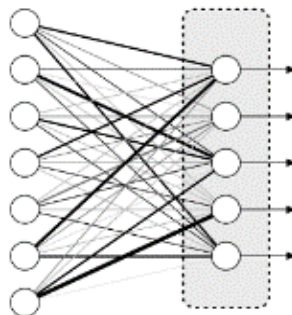


Figure 4.6: Fully Connected Layer

- **Dropout Layer**

Since the training process on CNN is done with big data, the network can sometimes memorize. The dropout layer can be used to prevent this memorization. The basic logic of this layer is to eliminate some knots (Özkan and Ülker 2017). Eliminating knots prevent units from adapting too much. This layer is known to be successful in preventing the overfitting problem. Figure 4.7 shows a dropout function scheme (Yasaka et al., 2018).

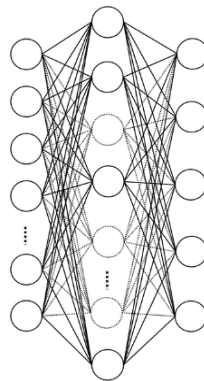


Figure 4.7: Dropout Function

4.2.1 AlexNet

Deep learning has made a great impact with its success in the world of science in 2012. CNN won the contest with great success in ImageNet, an ILSVRC in 2012. As the core architecture of deep learning, CNN has led to the rise of deep learning, by virtue of its winning the competition. In the competition, the error rate of 26.1% has shown its success by reducing it to 15.3% error rate with CNN. The AlexNet model, designed with a deep learning architecture, won the ImageNet competition in 2012 (Özkan and Ülker 2017).

Compared to machine learning and computer vision methods, AlexNet is an architecture that achieves high accuracy in terms of visual recognition. Deep learning has achieved a rapid rise in history through its classification and visual recognition ability with AlexNet (Alom et al., 2018). AlexNet has a complex and large dataset with 1000 classes and more than 1.2 million images. This dataset is called the ImageNet dataset. These are important criteria for computer vision techniques. The network architecture of this model includes the convolution

layer, pooling layer, and fully connected layers. It also includes DropOut and ReLu layers, which are network components of CNNs (Dourado et al., 2019).

AlexNet, designed by Krizhevsky, et al., is an eight-layer CNN model. (Krizhevsky et al., 2012). The purpose of an Alexnet structure is to classify 1000 class tags. In the first AlexNet architecture, the filter of the first layer, the convolutional layer, is fed with the input image (224x224x3) with 96 kernels of size (11x11x3) and a stride of 4 pixels. In the AlexNet architecture, which consists of many layers, the data from the first layer is normalized and fed into the second convolutional layer after pooling. The convolutional layer after the pooling layer uses 256 kernels (5x5x48) in size. Other convolutional layers in the architecture are interconnected. The third layer connects to the processed outputs of the second layer. This is 384 kernel sizes (3x3x256). The dimensions of the fourth and fifth convolutional layers, respectively; it has 384 core sizes (3x3x192) and 256 core sizes (3x3x192). The last layer, the fully connected layer, has 4096 neurons. AlexNet architecture has 650,000 neurons and 60,000,000 parameters. This network has 5 convolutional layers and a thousand-way softmax. After these layers, it has 3 fully connected layers. Maximum pooling layers can be found after some convolutional layers. AlexNet CNN architecture for image classification is successful compared to other methods (Krizhevsky et al., 2012). The AlexNet architecture has 8 layers with multiple and different functions. Of these 8 layers, 5 are convolutional layers. It is called conv1 to conv5. 3 layers are fully-connected layers. These are called fc6, fc7, and fc8 (Mesrabadi and Faez 2018). The figure 4.9 represents the layer structures of the AlexNet architecture, which uses filters of size 11x11 and the number of step shifts is 4 (Özkan and Ülker 2017).

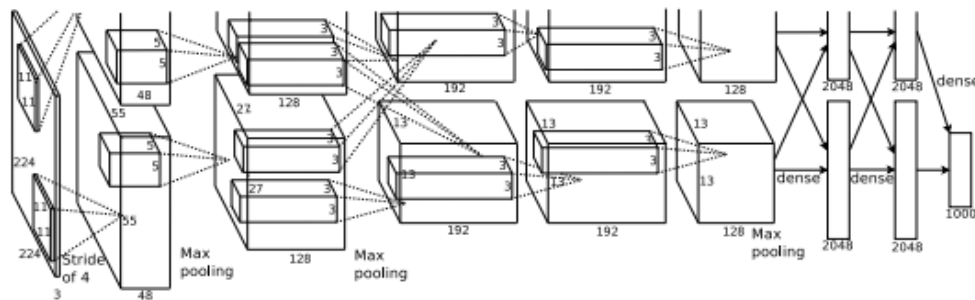


Figure 4.8: Structures of the AlexNet

Convolution layers in the AlexNet architecture can also be called feature extraction layers because of their function. There may be a pooling layer between two convolutional layers. This pooling layer reduces dimensionality, minimizing computational complexity. Maximum pooling and average pooling can be used in common pooling schemes. The maximum pooling layer calculates the largest value of the filtered image and can discard the noise data in the filtering window. AlexNet's first and second convolutional layers use 11x11 and 5x5 size filters. Filters in these layers are used for feature extraction. The other remaining convolutional layers use a 3x3 filter. Different filter sizes are used for different inputs. Fully connected layers perform of learning classification functions by taking the attribute vectors (Yuan et al., 2020). AlexNet, which has the ability to be trained with approximately one million images, has a high success in image classification (Toğaçar and Ergen 2018). Block diagram of the AlexNet model architecture is as depicted in Figure 4.9 (Beeharry and Bassoo 2020).

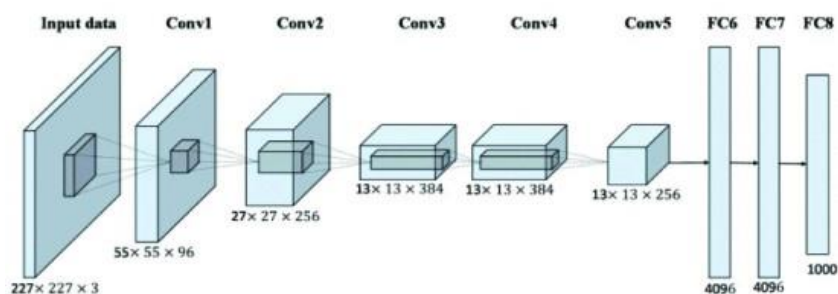


Figure 4.9: AlexNet Architecture

AlexNet uses some strategies to develop learning skill. It can do this by increasing network depth and using multi-parameter optimization methods. It was necessary to solve the problem of deep networks, their being trapped in gradient loss. AlexNet designers used activation functions to solve this problem. They used the ReLu function as the activation function (Lu et al., 2021). AlexNet's success has increased because it used the ReLu nonlinear layer and also used the dropout regularization technique. ReLu can speed up the

training phase of the network and prevent over-fitting (Han et al., 2017). The definition of ReLu is shown in equation 4.1.

Also, with the dropout layer that comes after full connections, overfitting can be prevented and adaptation between neurons can be reduced and robustness can be improved. (Lu et al., 2021). It is necessary to reduce the adaptation of neurons among themselves. For this, dropout layer is used after fully connected layers in AlexNet architecture. Dropout tries to set the input neurons or latent neurons to zero to reduce adaptations (Han et al., 2017). In the convolution layer, the complexity of the network can be reduced by the method of sharing parameters. Also, it can automatically learn, features from educational images. Equation 4.3 shows the definition of the convolution.

$$C(m, n) = (M * w)(m, n) = \sum_k \sum_l M(m - k, n - l)w(k, l) w(k, l) \quad (4.3)$$

Where (m, n) is the size of image M and (k, l) is the size of the convolution kernel w .

The pooling layer generally performs the feature reduction function. For the representation of pixels in the feature map created in the convolution layer, the pooling layer generates a value. Thus, feature maps are normalized before being fed to the next layer of the network. The direct connection of neurons with each other takes place in a fully connected layer. Neurons in the (0,1) range are activated using the softmax activation function. Representation of softmax activation function is given in equation 4.4.

$$softmax(X)_i = \frac{exp(x_i)}{\sum_{j=1}^n exp(x_j)} \quad (4.4)$$

Where $exp(x_i)$ Defines the normal exponential function applied to each component x_i of the input vector X , $\sum_{j=1}^n exp(x_j)$ is the standardization term, and n is the number of categories (Lu et al., 2021).

There are impressive features of the AlexNet architecture that make CNN so effective. For example, AlexNet uses ReLu. The activation function, ReLu, is useful in calculation as it only makes one comparison. AlexNet also prefers maximum overlapping pooling in the network architecture. At maximum pooling, the step size of the filtering medium is smaller

compared to the size of the filter. Another feature is the use of dropout technique, which assigns zero to the output value in order to reduce the problem of overfitting (Yuan et al., 2020).

Each layer of the AlexNet architecture has filters that can reduce noise and improve features. The pooling layer that follows the convolution layer allows the number of features to be reduced and can only extract essential features. Also, as an activation function; ReLu, which increases the probability of gradient disappearance compared to functions such as sigmoid, tanh, arctan, is used in AlexNet. It has been found that AlexNet has faster processing capability compared to other deep architectures. Compared to other deep architectures that require special hardware, AlexNet works well, with GPU and hardware limitations (Hosny et al., 2020).

4.2.2 ResNet-101

The success and superiority of deep network architectures has been reported, in many studies in recent years. The researchers were inspired by ImageNet's deepest architecture and design the Residual Network (ResNet-101) (Iqbal et al., 2021). Residual Network is named ResNet-101 for short. Deep convolution networks are known to be successful for image classification processes. Generally, convolutional neural networks are tried to be deepened to increase the accuracy of classification processes. However, as deepening increases, training of the neural network can become difficult as the gradient will disappear with back propagation. Residual learning focuses on solving such problems. It consists of stacked layers of a deep CNN. Trainings using the ResNet architecture are more effective than deep CNNs training. ResNet uses jump links so that gradients are not lost (Gupta et al., 2021)

ResNet-101 architecture layers, a CNN model, are used for classification and feature extraction, reduction. These layers consist of the convolution layer, pooling layer and fully connected layers (Ali et al., 2021). ResNet, which means residual networks, has an important use in computer vision problems. By applying the chain rule, the gradients being zero problem can be solved with the ResNet network. This network uses orphaned connections to which gradients will be passed directly (Demir et al., 2019). ResNet is a different model due to the greater depth of the network compared to other models. In the ResNet network,

blocks feed the layers that come after them. The residual values of these blocks are added to the model. By means of this feature, ResNet is different from other models. The added value in the two layers between the Linear and ReLu layers changes the calculations in the network (Yıldırım and Dandıl 2020).

The development of 50-layer ResNet is a residual network called 101-layer ResNet-101 (Ghosal et al., 2019). The convolutional neural network, called ResNet-101, consists of 101 deep layers and allows the data to be classified. The figure 4.10 shows a ResNet-101 architecture (Tahir et al., 2021).

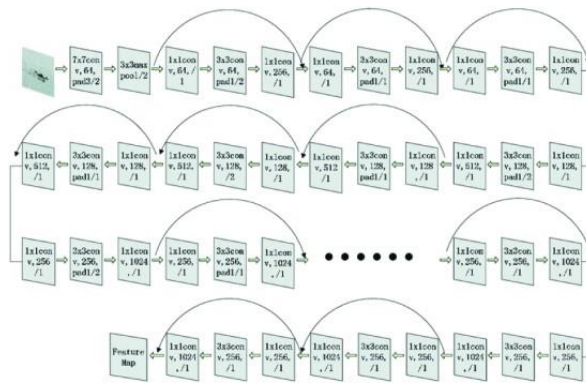


Figure 4.10: ResNet-101 Architecture

The ResNet model is utilized by setting the input images size to 224×224 , a well-trained ResNet-101 network classifies new data collected from the input images (Ali et al., 2021; Zhao et al., 2021). In CNN architectures, some layers are often interconnected and trained to perform various operations. At the end of the operations performed on the layers, different features are learned by the network. In the ResNet architecture, the layers have a number of filters to be the same as the size of the feature map in the output. However, to maintain the complexity of time, the number of filters is doubled in each layer when the size of the feature map is halved. It folds these layers in two steps to directly execute subsampling. It ends with the last layer of the ResNet architecture, the average pool layer and the fully connected layer enabled by softmax. Residual learning can easily interpret the extraction of input properties from the fully connected layer. ResNet makes this interpretation using the shortcut

connections for every 33 pairs of filters. In order to prevent the gradients from disappearing, the activation functions in the preceding layer are reused to learn the weights in the current layer. Therefore, layers are bypassing. Weights are adjusted to strengthen the layer next to the current layer and mute the previous layer to train the network. This ResNet network is easier to train than to train other CNN networks. ResNet also solves the problem of accuracy drops (Ghosal et al., 2019).

ResNet-101 network architecture has convolution layer, pooling layer, fully connected layer and softmax layer. A block diagram of the ResNet architecture is shown in the figure 4.11. As shown in this figure, the dimensions are increased by using shortcut connection, then the convolutional layer depth is increased to improve model performance. Increasing the network depth with a shortcut will result in a corruption problem. To solve the corruption problem, shortcut connections perform identity mapping. These shortcut connections do not cause calculation complexity or adding additional parameters. The ResNet-101 network can be trained end-to-end. This training can be trained using stochastic gradient descent (SGD) via back propagation (Zhao et al., 2021).

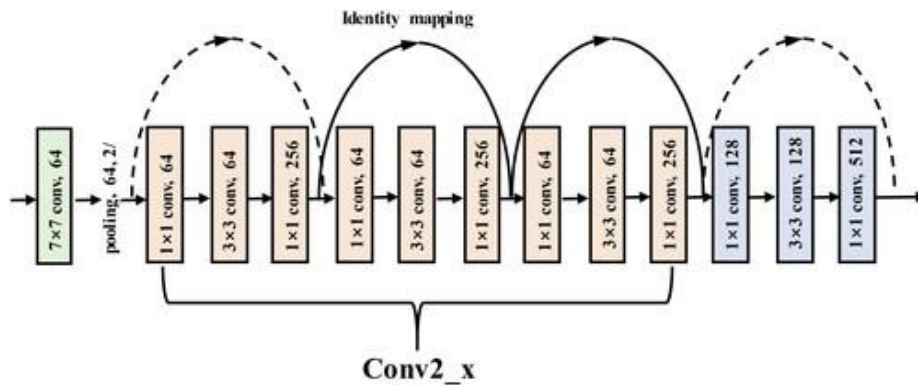


Figure 4.11: Shortcut connections of ResNet-101

ResNet-101, learns identity connections, incremental and residual representations. This learning creates a path for backpropagation. If the parameters of the $f(x)$ part start at or near zero, the identity layers change from simple to complex. The training difficulty of deep networks caused by gradient loss is tried to be solved with residual blocks. The ResNet-101

architecture uses a 3x3 filters stride of two and a 3x3 maximum pooling layer with a stride of two (Zheng et al., 2021).

In the ResNet-101 network, the same number of layers and the same number of filters are used, for the same output characteristics. Integration chain is used in ResNet-101 and residual connection is used after this application. Residual networks consist of selected units. Each unit can be represented as follows;

$$y_i = h(a_i) + F(a_i, w_i) \quad (4.5)$$

And

$$a_{i+1} = F(y_i) \quad (4.6)$$

a_i represents the input, $F(a_i, W_i)$ residual function $a_{(i+1)}$ depends on y_i , so $a_{(i+1)}$ is the output.

Residual network can be represented by the following formula; $F = W_i \delta(W_i a)$

Linear projection (W_m) is used to match the dimensions when the dimensions of a_i and y_i are not equal. Or W_m is used to equalize the dimensions when the input and output channels are swapped.

$$y_i = F(a_i, W_i) + W_m a \quad (4.7)$$

The residual function $F(a_i, W_i)$ represents multiconvolution layers. ResNet-101 can be written repeatedly.

$$x_l = x_i + \sum_{n=i}^l -1 F(a_i, W_i) \quad (4.8)$$

(Iqbal et al., 2021)

ResNet-101 has some advantages thanks to its deeper structure compared to other models. ResNet-101 has better feature extraction ability from image data. ResNet offers to skip the

connection. Because it allows moving the entry from the previous layer to the next layer without changing the input (Taş and Yılmaz, 2021).

4.2.3 Inception-V3

Since 2015, the Google research team and Szegedy et al. have studied complex networks and have introduced many versions of complex networks called the Inception module. The Inception module is focused on increasing the depth and width of the network. In doing so, while improving the classification performance of very deep convolutional networks, it's maintaining the computational resources of networks at the same layer (Al-Masni et al., 2020).

In 2015, a 48-layers Inception-V3 model was proposed, which is an improved form of the GoogleNet design (Mednikov et al., 2018). Inception-V3 has been trained with multiple images from the ImageNet data source. It is an advanced CNN model, also called GoogleNet (Khamparia et al., 2020). Inception-V3 is a well-known image recognition model that is 48 layers deep and has been generally used to achieve great exactness on the results of ImageNet dataset. The Inception-V3 model is utilized by setting the input images size to 299*299. The Inception-V3 network has been trained with over one million images on ImageNet. This trained network can categorize images into a thousand objects (Vidyarthi et al., 2020). A 22-layer network was first introduced in 2015 with the name GoogleNet or Inception-V1. Inception-V3 is the deep network architecture that is the third upgrade of the Inception-V1 model introduced. Inception-V1 was first upgraded to Inception-V2 by batch normalization. Later, it was promoted to Inception-V3 with additional factorization (Vidyarthi et al., 2021). Inception-V3 network architecture is represented in Figure 4.12 (Dong et al., 2020).

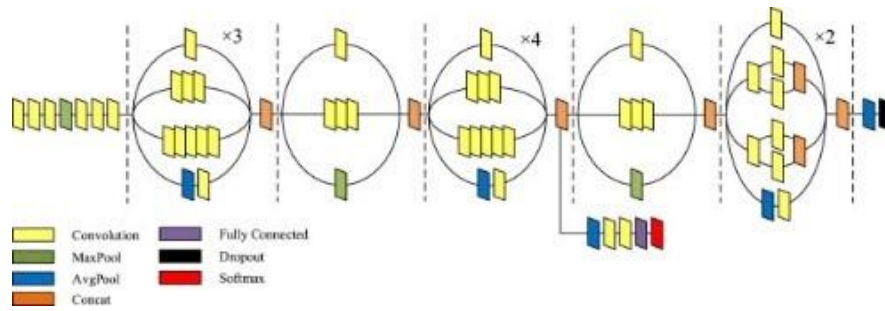


Figure 4.12: Inception-V3 Network Architecture

The Inception-V3 model is a CNN model that extends the architecture by combining factorization ideas to reduce the number of parameters and connections without reducing the efficiency of the network (Boussaad and Boucetta, 2020). The model carries out convolution factorization what separates two-dimensional convolutional kernels to one-dimensional kernels. The model is based on symmetric and asymmetric blocks, including convolutions, average pooling, max pooling, concats, dropouts, and fully connected layers (Vidhyarthi et al., 2020). Figure 4.13 represents a block diagram of the Inception-V3 module, which incorporates convolution layer, pooling layer, and on the last layer is Softmax classifier which can be adjustable dependent on the disposition of the classification problem (Nguyen et al., 2018).

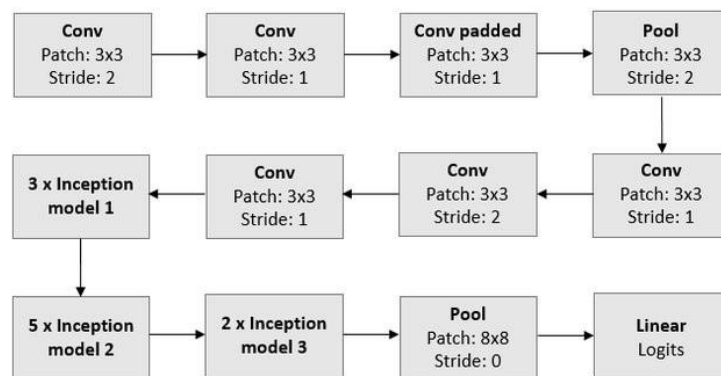


Figure 4.13: An architecture of the Inception-V3 module

Layers have been created to maximize the flow of information to the Inception-V3 network. This architecture creating layers by carefully constructing networks, balance depth and width of the network (Radhika et al., 2020). Inception-V3 is focused on reducing the parameter set. It can do this by separating large convolution layers into smaller convolution layers (Sundar et al., 2018). Inception-V3 architecture has one helper classifier and this auxiliary classifier acts as a regulator (Alzubaidi et al., 2021).

Compared to the Inception V1 and V2 models, the Inception-V3 model uses the convolution kernel division method. This method breaks large volume integrals into small convolutions. With this division method, it is aimed to reduce the number of parameters. In this way, the spatial feature can be extracted more effectively and the training speed can be accelerated (Dong et al., 2020). Inception-V3 architecture is a deep CNN and has been intended to perform computational estimations effectively utilizing 12 times fewer parameters than different models. In this way, this architecture is allowed to be applied to less powerful systems (Quiñonez et al., 2019). Inception-V3 has a few upgrades like factorized convolutions, assistant classifiers, and effective grid size-decrease to reduce the complete number of parameters and computational complexity (Ayan et al., 2020).

The benefit of Inception-V3 is to increase the compute capacity of the network, to increase the depth of the network and to increase the nonlinear of the network (Li et al., 2018). The Inception-V3 networks has the capacity to recognize wider scope of images instead of go deeper into networks. Its capacity to include various small convolutions with restricted parameters types and size as opposed to bigger filter size convolutions, lastly concatenate them make it unique in relation to others. Through usage of such a network, various filters of different sizes combined into a new single filter which reduces the convolutional filter size as well as reduces the general network computational complexity. The Inception-V3 architecture is illustrated in Figure 4.14 (Khamparia et al., 2020).

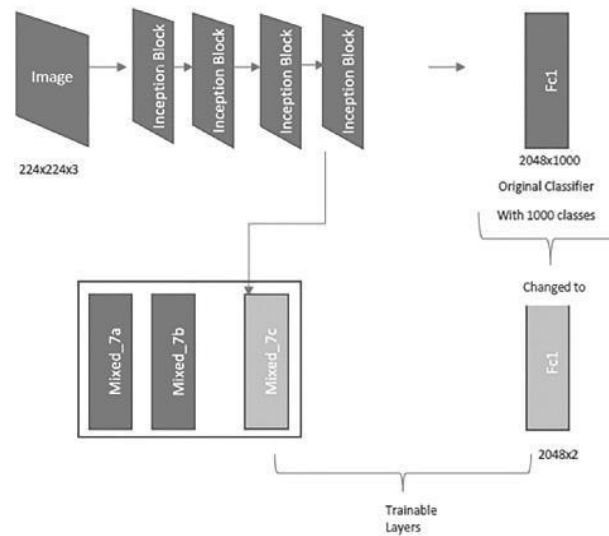


Figure 4.14: Architecture of Inception-V3

4.2.4 EfficientNet-B0

EfficientNet was proposed by Google in 2019 which has extraordinary ability of feature extraction. Compared to other CNNs, EfficientNet-B0 architecture has fewer parameters and higher accuracy values. The network of EfficientNet is planned utilizing a multiobjective neural architecture search, and afterward, the baseline network is scaled as far as depth, width, and resolution to accomplish a balance among them (Su and Wang 2020). EfficientNet networks are one of the most recently developed networks among visual object recognition methods. EfficientNet's have 8 different versions. These are architectures starting with EfficientNet-B0 up to EfficientNet-B7. EfficientNet designs are based on neural networks architecture. EfficientNet has fewer parameters and smaller scale compared to other networks. This network is successful in image classification tasks (Huynh et al., 2020).

The basis of the EfficientNet-B0 model is based on the deep learning algorithm CNN. EfficientNet-B0 generally takes into consideration parameters such as calculation cost, speed, usability and accessibility (Altan and Karasu, 2020). EfficientNet can be thought of as a group of CNN models. Looking at some details, EfficientNet-B0 is more efficient than other models. EfficientNets depend on AutoML and compound scaling to accomplish superior execution without compromising resource effectiveness. AutoML Mobile structure

EfficientNet architecture has a convolution layer. This layer has 3x3 mobile inverted bottleneck convolution (MBConv) blocks and different kernel sizes. In addition, this model provides high accuracy and can also be scaled successfully (Pham et al., 2020). The EfficientNetB0 model uses MBConv and also uses multiple convolutional layers. Feature extraction is done using these layers. EfficientNetB0 features balanced depth, width, and resolution. With these features, it has become a scalable, accurate, and easily deployable model. Compared to other CNN models, EfficientNet-B0 uses a fixed set of scaling coefficients. It can scale any dimension using these sets of coefficients. Thanks to this feature, it has been more successful than other models trained in the ImageNet dataset. In addition, it has achieved successful results on the ImageNet data set in transfer learning. Researchers and developers can access and provide computing that has been successful with EfficientNets deep learning capabilities (Montalbo and Alon 2021).

The EfficientNet-B0 model is utilized by setting the input images size to 224×224 (Müftüoğlu et al., 2020). The littlest and baseline model EfficientNet-B0 comprises 5.3 millions number of parameters and 0.39 billions of FLOPS (Floating Point Operations Per Second) (Duong et al., 2020). Specifically, the baseline model EfficientNet-B0 comprises 18 layers. The other EfficientNet models, i.e., B1 ÷ B7 are scaled up from the standard EfficientNet-B0 with various compound coefficients (Duong et al., 2020).

EfficientNet-B0 models depend more on baselines. There are more layers of abstraction and tighter end-to-end integration training. In this way, EfficientNet-B0 models can achieve success. However, EfficientNet-B0 has a lack of interpretability. The interpretability feature increases the transparency of the model and increases reliability. Conventional interpretable algorithms depend on rules or expert systems. They give each section an intuitive interpretation through manual designs however not accurate. The figure 4.16 shows the EfficientNet-B0 network model. (Hu et al., 2020).

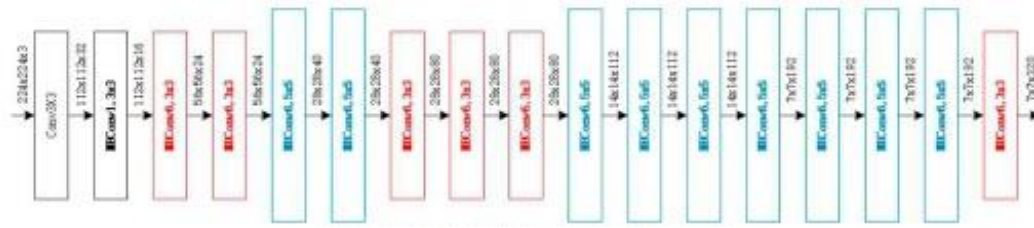


Figure 4.16: EfficientNet-B0 Network Model

The EfficientNet-B0 model is smaller compared to other ImageNet successful models. Compared to the ResNet-50, which has a total of 23.5 million parameters, the EfficientNet-B0 model contains 5.3 million parameters. So with EfficientNet-B0, the parameter has been significantly reduced (Hussain et al., 2021).

4.2.5 NasNet-Mobile

NAS represents Neural Architecture Search and is a programmed automatic design for designing artificial neural networks (Schneider et al., 2021). NAS is an algorithm that characterizes the building blocks that can be used to build its network and looks for the best neural network architecture. In this algorithm, a regulator, recurrent neural network (RNN), samples these structure blocks, assembling them to make some sort of end-to-end architecture. In the NASNet, the NAS algorithm finds how to put together structure blocks (Bahri et al., 2019). Block diagram of the NasNet model architecture is as depicted in Figure 4.17 (Radhika et al., 2020).

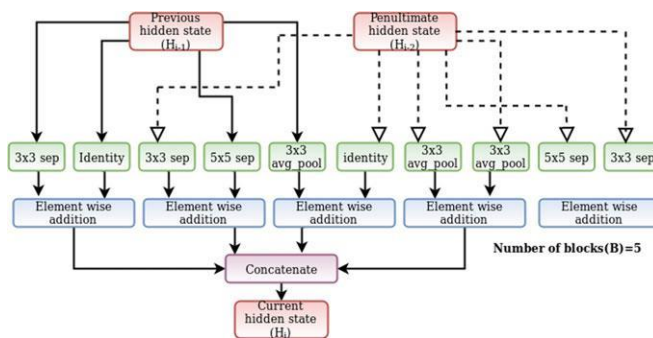


Figure 4.17: NASNet Architecture

NASNet has two different models, specifically, large and mobile. The NasNet-Mobile model has significantly fewer parameters compared to the large model, just 4 million in examination with the 84 million for the Large (Bahri et al., 2019). NasNet-Mobile design was created to move this network to a larger data set after creating a network in a small data set. NAS was used to do this (Trong et al., 2020). The NasNet architecture used a 331x331 size input image to train the NasNet Large model. NasNet-Mobile architecture is trained with 224x224 size entrance image. The NasNet-Large model has more parameters than NasNet-Mobile. With fewer parameters, NasNet-Mobile is more reliable (Radhika et al., 2020).

An architecture was designed that can create a neural network with machine learning techniques based on a specific dataset, an AutoML technique created by Google researchers. This design is called Neural Architecture Search Network (NasNet). This designed system transfers the best architecture learned in small datasets such as AutoML and CIFAR10 to the ImageNet dataset (Toraman et al., 2019). NasNet-Mobile architecture is proposed by Google Brain. This architecture can create a smaller size model thanks to smaller floating-point operations. This model is an architecture that performs better compared to previous models. The NAS network is based on reinforcement learning search. Searches cells in a smaller data set (Singh et al., 2021). NasNet-Mobile structure uses RNNs in training repetition and different architectures are created. These networks created later are trained. Accuracies are created in the trained networks verification data set. Then the update is performed depending on the controller RNN accuracies (Zhang et al., 2019).

NasNet architecture, which uses reinforcement learning, was created with neural architecture research, consists of the building block cells it defined, and is a scalable CNN architecture. A cell consists of convolution and pooling layers. It can also be repeated many times, depending on the requirements of the network. The NasNet-Mobile model includes 5.3 million parameters. This model also has 564 million multi-accumulates (MACs) 12 cells (Saxen et al., 2019). NasNet-Mobile contains two types of convolutional cells. These are successively reproducible normal and reduction cells. Both of these cells use the NasNet-Mobile network for transfer learning. They can also create feature maps (Linkon et al., 2020).

NasNet-Mobile design consists of several layers. These layers are; convolution layer, pooling layer, and the bulk normalization layer. It also has this architecture, building blocks. Reinforcement learning is used to optimize these blocks. This process is repeated several times depending on the capacity of the network (Khan et al., 2021). NasNet-Mobile is a deep network. The task of the first layers of this architecture is to extract low-level features, independent of data such as edges. Thus, first layer weights can be used in all applications. However, the weights of the last layer are set dependent on the network data set and cannot be used in other applications. Therefore, the stochastic gradient descent (SGD) algorithm is used as an optimizer. In addition, because the network is deep, it is a high probability that the network overfits (Bahri et al., 2019).

NasNet-Mobile is a model with the lowest computational complexity architecture (Toraman et al., 2019). Also, NasNet-Mobile is a lightweight model and requires a small amount of GPU memory (Pérez et al., 2021).

4.3 Database

Deep networks need a lot of data to provide high performance. Therefore, a good database with a large number of normal and abnormal images is needed to train and test the developed network. All of the images in this study were courtesy of CT images were obtained from the database with the approval of Dr. Burhan Nalbantoğlu Hospital ethics committee. This database includes abdominal CT images and is in cross-section. The number of slices of each patient scan used in this study ranged from 55 to 110. These images were labeled by the radiologist as images with and without kidney stones to train the network. Images are in JPEG format and abdominal CT images of 30 patients with stones and 30 patients without stones were used (Table 4.1).

Table 4.1: Dataset

Image set	Number Patient	Number Images
Including kidney stone	30	2760
Not including kidney stone	30	2749

Both	60	5509
-------------	----	------

Figure 4.17 shows a sample of the abdominal CT images found in the database used for training and testing the employed models. Note that the figure shows the two classes of the database images: the non-stone and the stone.

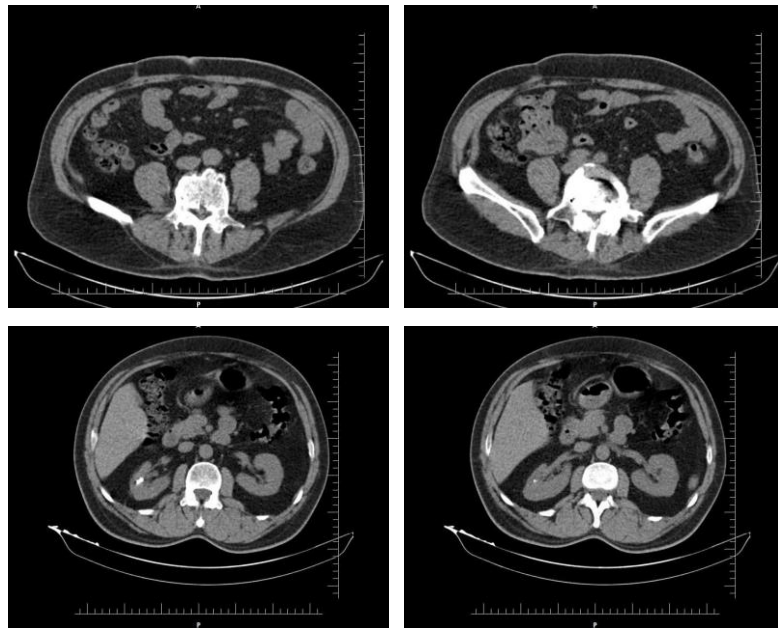


Figure 4.18: Images of database, CT abdominal patient samples

A database of abdominal CT scans of a total of 60 patients was used for training and testing. In this study, out of a total of 5,509 images; Random 25%, ie 1,162 images were reserved for testing and 4,347 images were used for training. Results could change if the number of images reserves for training and testing changed. However, training on a higher number of images is more important. Table 4.2 shows the number of images found in the database to be used for training and testing.

Table 4.2: Dataset and data division

Image set	Patients Number	Number images	Number images	Number of images without kidney stone
Training set	48	4347	2178	2169
Testing set	12	1162	571	591
Both set	60	5509	2749	2760

4.4 Algorithm of the Applied Methods

This study presents an original investigation for the classification of kidney stones from CT images using deep learning algorithms.

5 different CNN models based on deep learning are selected for classification. These are; AlexNet, ResNet-101, Inception-V3, EfficientNet-B0, NasNet-Mobile. Matlab programming language was used for the training and testing of 5 CNN models.

The step by step procedure can be listed as:

1. Initially a strong database is formed using expert radiologist to label every image. Then database is divided into training and testing subsets.
2. Images in the database resized for every deep learning framework.
3. Transfer learning method is applied to every framework to be tailored for the task. The output layer value of each network has been changed.
4. The selected deep learning framework trained separately by using the training data and as a result the performances are recorded.
5. After the training stage for every framework completed, they are tested with the testing data.
6. Finally Testing Accuracy, Sensitivity and Specificity measures are calculated for every network to evaluate the overall performance of the project. (Equations 4.9, 4.10 and 4.11)

To calculate the sensitivity: we take the ratio of true positive images with kidney stones divided by the summation of the number of test images for true positive with kidney Stones and false negative images with kidney stones. Equation 4.9 shows the calculation on sensitivity.

$$\frac{\textit{true positive}}{(\textit{true positive} + \textit{false negative})} \quad (4.9)$$

To calculate the specificity: we take the ratio of true negative images without Kidney stone divided by the summation of the number of test images for true negative without Kidney stone and false positive images without Kidney stones. Equation 4.10 shows the calculation on specificity.

$$\frac{\textit{true negative}}{(\textit{true negative} + \textit{false positive})} \quad (4.10)$$

To calculate the test accuracy: we take the ratio summation of true positive and true negative images divided by the summation of the all test images. Equation 4.11 shows the calculation on test accuracy.

$$\frac{(\textit{true positive} + \textit{true negative})}{(\textit{true positive} + \textit{false negative} + \textit{false positive} + \textit{true negative})} \quad (4.11)$$

CHAPTER 5

RESULTS

In this section, the results obtained for the applied deep learning methods in section 4.4 for the classification of kidney stones are presented in detail.

In this study, CT abdominal images obtained from 60 patients were classified using several state of the art deep learning based CNN models.

A total of 5509 images were used, 2760 of them containing kidney stone and 2749 of them are without kidney stone.

Table 5.1 shows the performance measures obtained for training and testing of each different deep learning framework.

Table 5.1: Performance Results

Network	Training accuracy %	Test accuracy %	Sensitivity %	Specificity %
AlexNet	67.00	64.11	65.14	63.05
ResNet-101	78.30	77.54	77.16	77.93
Inception-V3	74.00	75.48	73.60	75.48
EfficientNet-B0	76.61	78.40	76.14	80.74
NasNet-Mobile	74.62	73.84	73.10	74.61

As observed from Table 5.1; when training accuracies are compared ResNet-101 obtained the highest performance for the given task, EfficientNet-B0 coming second. AlexNet obtained the worst training performance.

When testing accuracies are evaluated, this time EfficientNet-B0 obtained the highest performance while ResNet-101 coming second. Again AlexNet obtained the worst result suggesting it is not quite suitable for the given task. Improvement in the fine tuning procedures during transfer learning can improve the overall performances of these networks.

Following their training and testing performances, EfficientNet-B0 and ResNet-101 also obtained the best sensitivity and specificity performances suggesting that they are the most suitable frameworks for our transfer learning based kidney stone classification task.

5 deep learning methods are successfully applied in this project to evaluate their performances for the task of transfer learning based classification of kidney stones from patient CT scans.

CHAPTER 6

CONCLUSION

Kidney stone disease is known to be a common disease affecting about 1 in 10 people. The fact that it is accepted as both a chronic and systemic disease reveals the degree of effect of the disease. As with any disease, it is very important to detect kidney stone correctly. CT scanners used to view kidney stones are a common imaging method. In particular, the diagnosis of kidney stone disease, understanding the composition of kidney stones, their location in the kidney area, the density and size of the stones are the information that should be obtained for disease management and treatment. By scanning the kidneys with CT, this information can be accessed accurately due to the high sensitivity of CT. According to this information about stones in the kidney, the correct treatment method is determined by the doctors. In this way, information about the degree of the disease can be obtained during and after the treatment.

Although CT scanners provide highly accurate information about kidney stones, multiple slices of images are manually reviewed by radiologists to assess the disease. This process is laborious and time-consuming. Radiologists analyse CT images by eye ball estimation, because of the manual analysis human errors can be occurred.

Deep learning algorithms have gained popularity thanks to their high performance in medical image analysis as well as in many applications. This study focused on classifying kidney stone images obtained from CT scans with deep learning algorithms.

Automatic classification of kidney stone disease with deep learning can provide technical support to radiologists as well as assist existing medical specialist in classification in regions where there is no expert access. In this study 5 deep learning based CNN models are used to classify kidney stones. Acceptable performances of each CNN model in classifying kidney stones were obtained.

The raw data obtained from CT scans can be cited as the limitation of this study. CNN models had difficulties in the training phase because raw data was used. Small stones in our database reduce the classification accuracy. In future studies, some extractions can be made in the database to achieve higher performance and the data can be improved. In addition, the

proposed models can be tested using different abdominal datasets. The existing database can be trained with different CNN models. In future studies, the composition or size of kidney stones can be determined with CT images.

REFERENCES

- Akay, A., & Hess, H. (2019). Deep learning: current and emerging applications in medicine and technology. *IEEE journal of biomedical and health informatics*, 23(3), 906-920.
- Akshaya, M., Nithushaa, R., Raja, N. S. M., & Padmapriya, S. (2020, July). Kidney Stone Detection Using Neural Networks. In *2020 International Conference on System, Computation, Automation and Networking (ICSCAN)* (pp. 1-4). IEEE.
- Albawi, S., Mohammed, T. A., & Al-Zawi, S. (2017, August). Understanding of a convolutional neural network. In *2017 International Conference on Engineering and Technology (ICET)* (pp. 1-6). Ieee.
- Alelign, T., & Petros, B. (2018). Kidney stone disease: an update on current concepts. *Advances in urology*, 2018.
- Ali, S., Hassan, M., Saleem, M., & Tahir, S. F. (2021). Deep transfer learning based hepatitis B virus diagnosis using spectroscopic images. *International Journal of Imaging Systems and Technology*, 31(1), 94-105.
- Al-Masni, M. A., Kim, D. H., & Kim, T. S. (2020). Multiple skin lesions diagnostics via integrated deep convolutional networks for segmentation and classification. *Computer methods and programs in biomedicine*, 190, 105351.
- Alom, M. Z., Taha, T. M., Yakopcic, C., Westberg, S., Sidike, P., Nasrin, M. S., ... & Asari, V. K. (2018). The history began from alexnet: A comprehensive survey on deep learning approaches. *arXiv preprint arXiv:1803.01164*.
- Altaf, F., Islam, S. M., Akhtar, N., & Janjua, N. K. (2019). Going deep in medical image analysis: concepts, methods, challenges, and future directions. *IEEE Access*, 7, 99540-99572.
- Altan, A., & Karasu, S. (2020). Recognition of COVID-19 disease from X-ray images by hybrid model consisting of 2D curvelet transform, chaotic salp swarm algorithm and deep learning technique. *Chaos, Solitons & Fractals*, 140, 110071.

- Alzubaidi, F., Mostaghimi, P., Swietojanski, P., Clark, S. R., & Armstrong, R. T. (2021). Automated lithology classification from drill core images using convolutional neural networks. *Journal of Petroleum Science and Engineering*, 197, 107933.
- Andrabi, Y., Patino, M., Das, C. J., Eisner, B., Sahani, D. V., & Kambadakone, A. (2015). Advances in CT imaging for urolithiasis. *Indian journal of urology: IJU: journal of the Urological Society of India*, 31(3), 185.
- Ayan, E., Erbay, H., & Varçın, F. (2020). Crop pest classification with a genetic algorithm-based weighted ensemble of deep convolutional neural networks. *Computers and Electronics in Agriculture*, 179, 105809.
- Bahri, A., Majelan, S. G., Mohammadi, S., Noori, M., & Mohammadi, K. (2019). Remote sensing image classification via improved cross-entropy loss and transfer learning strategy based on deep convolutional neural networks. *IEEE Geoscience and Remote Sensing Letters*, 17(6), 1087-1091.
- Beeharry, Y., & Bassoo, V. (2020, November). Performance of ANN and AlexNet for weed detection using UAV-based images. In *2020 3rd International Conference on Emerging Trends in Electrical, Electronic and Communications Engineering (ELECOM)* (pp. 163-167). IEEE.
- Black, K. M., Law, H., Aldouhki, A., Deng, J., & Ghani, K. R. (2020). Deep learning computer vision algorithm for detecting kidney stone composition. *BJU international*.
- Boussaad, L., & Boucetta, A. (2020). Deep-learning based descriptors in application to aging problem in face recognition. *Journal of King Saud University-Computer and Information Sciences*.
- Briggs, J. P., Kriz, W., & Schnermann, J. B. (2009). Overview of kidney function and structure. *Primer on Kidney Diseases*, 2-18.
- Brisbane, W., Bailey, M. R., & Sorensen, M. D. (2016). An overview of kidney stone imaging techniques. *Nature Reviews Urology*, 13(11), 654.
- Chen, W., Qiu, Y., Feng, Y., Li, Y., & Kusiak, A. (2021). Diagnosis of wind turbine faults with transfer learning algorithms. *Renewable Energy*, 163, 2053-2067.

- Clarkson, M. R., Brenner, B. M., & Magee, C. (2010). *Pocket companion to brenner and rector's the kidney E-Book*. Elsevier Health Sciences.
- Coe, F. L., Evan, A., & Worcester, E. (2005). Kidney stone disease. *The Journal of clinical investigation*, *115*(10), 2598-2608.
- Cui, Y., Sun, Z., Ma, S., Liu, W., Wang, X., Zhang, X., & Wang, X. (2020). Automatic Detection and Scoring of Kidney Stones on Noncontrast CT Images Using STONE Nephrolithometry: Combined Deep Learning and Thresholding Methods. *Molecular Imaging and Biology*, 1-10.
- Curhan, G. (2014). Nephrolithiasis. *National Kidney Foundation Primer on Kidney Diseases*, 405–411.
- Demir, A., Yilmaz, F., & Kose, O. (2019, October). Early detection of skin cancer using deep learning architectures: Resnet-101 and inception-v3. In *2019 Medical Technologies Congress (TIPTEKNO)* (pp. 1-4). IEEE.
- Dhar, M., & Denstedt, J. D. (2009). Imaging in diagnosis, treatment, and follow-up of stone patients. *Advances in chronic kidney disease*, *16*(1), 39-47.
- DOĞAN, F., & TÜRKOĞLU, İ. (2019). Derin Öğrenme Modelleri ve Uygulama Alanlarına İlişkin Bir Derleme. *Dicle Üniversitesi Mühendislik Fakültesi Mühendislik Dergisi*, *10*(2), 409-445.
- Dong, N., Zhao, L., Wu, C. H., & Chang, J. F. (2020). Inception v3 based cervical cell classification combined with artificially extracted features. *Applied Soft Computing*, *93*, 106311.
- Dourado Jr, C. M., da Silva, S. P. P., da Nobrega, R. V. M., Barros, A. C. D. S., Reboucas Filho, P. P., & de Albuquerque, V. H. C. (2019). Deep learning IoT system for online stroke detection in skull computed tomography images. *Computer Networks*, *152*, 25-39.
- Duong, L. T., Nguyen, P. T., Di Sipio, C., & Di Ruscio, D. (2020). Automated fruit recognition using EfficientNet and MixNet. *Computers and Electronics in Agriculture*, *171*, 105326.

- Ebrahimi, S., & Mariano, V. Y. (2015). Image quality improvement in kidney stone detection on computed tomography images. *Journal of image and graphics*, 3(1), 40-46.
- Edvardsson, V. O., Goldfarb, D. S., Lieske, J. C., Beara-Lasic, L., Anglani, F., Milliner, D. S., & Palsson, R. (2013). Hereditary causes of kidney stones and chronic kidney disease. *Pediatric nephrology*, 28(10), 1923-1942.
- Eisner, B. H., McQuaid, J. W., Hyams, E., & Matlaga, B. R. (2011). Nephrolithiasis: what surgeons need to know. *American Journal of Roentgenology*, 196(6), 1274-1278.
- Erickson, B. J., Korfiatis, P., Kline, T. L., Akkus, Z., Philbrick, K., & Weston, A. D. (2018). Deep learning in radiology: does one size fit all?. *Journal of the American College of Radiology*, 15(3), 521-526.
- Espinosa, G., & Esposito, R. (2020). Kidney Stones. In *Textbook of Natural Medicine* (pp. 1518-1527.e3).
- Evan, A. P. (2010). Physiopathology and etiology of stone formation in the kidney and the urinary tract. *Pediatric Nephrology*, 25(5), 831-841.
- Ghosal, P., Nandanwar, L., Kanchan, S., Bhadra, A., Chakraborty, J., & Nandi, D. (2019, February). Brain tumor classification using ResNet-101 based squeeze and excitation deep neural network. In *2019 Second International Conference on Advanced Computational and Communication Paradigms (ICACCP)* (pp. 1-6). IEEE.
- Graham-Knight, J. B., Scotland, K., Wong, V. K., Djavadifar, A., Lange, D., Chew, B., ... & Najjaran, H. (2019, December). Accurate Kidney Segmentation in CT Scans Using Deep Transfer Learning. In *International Conference on Smart Multimedia* (pp. 147-157). Springer, Cham.
- Gupta, A., Gupta, S., & Katarya, R. (2021). InstaCovNet-19: A deep learning classification model for the detection of COVID-19 patients using Chest X-ray. *Applied Soft Computing*, 99, 106859.
- Han, X., Zhong, Y., Cao, L., & Zhang, L. (2017). Pre-trained alexnet architecture with pyramid pooling and supervision for high spatial resolution remote sensing image scene classification. *Remote Sensing*, 9(8), 848.

- Hosny, K. M., Kassem, M. A., & Fouad, M. M. (2020). Classification of Skin Lesions into Seven Classes Using Transfer Learning with AlexNet. *Journal of Digital Imaging*, 33(5), 1325-1334.
- Hu, Q., Yin, S., Ni, H., & Huang, Y. (2020). An End to End Deep Neural Network for Iris Recognition. *Procedia Computer Science*, 174, 505-517.
- Hussain, N., Farooque, A. A., Schumann, A. W., Abbas, F., Acharya, B., McKenzie-Gopsill, A., ... & Cheema, M. J. (2021). Application of deep learning to detect Lamb's quarters (*Chenopodium album* L.) in potato fields of Atlantic Canada. *Computers and Electronics in Agriculture*, 182, 106040.
- Huynh, M. H., Pham-Hoai, P. T., Tran, A. K., & Nguyen, T. D. (2020, November). Automated Waste Sorting Using Convolutional Neural Network. In *2020 7th NAFOSTED Conference on Information and Computer Science (NICS)* (pp. 102-107). IEEE.
- Ibrahim, E. S. H., Cernigliaro, J. G., Pooley, R. A., Bridges, M. D., Giesbrandt, J. G., Williams, J. C., & Haley, W. E. (2016). Detection of different kidney stone types: an ex vivo comparison of ultrashort echo time MRI to reference standard CT. *Clinical imaging*, 40(1), 90-95.
- Iqbal, S., Siddiqui, G. F., Rehman, A., Hussain, L., Saba, T., Tariq, U., & Abbasi, A. A. (2021). Prostate Cancer Detection Using Deep Learning and Traditional Techniques. *IEEE Access*, 9, 27085-27100.
- Jubair, F., Al-karadsheh, O., Malamos, D., Al Mahdi, S., Saad, Y., & Hassona, Y. (2021). A novel lightweight deep convolutional neural network for early detection of oral cancer. *Oral Diseases*.
- Kaur, R., & Juneja, M. (2018). Comparison of different renal imaging modalities: an overview. *Progress in intelligent computing techniques: theory, practice, and applications*, 47-57.
- Ker, J., Wang, L., Rao, J., & Lim, T. (2017). Deep learning applications in medical image analysis. *Ieee Access*, 6, 9375-9389.

- Khamparia, A., Singh, P. K., Rani, P., Samanta, D., Khanna, A., & Bhushan, B. (2020). An internet of health things-driven deep learning framework for detection and classification of skin cancer using transfer learning. *Transactions on Emerging Telecommunications Technologies*, e3963.
- Khan, M. A., Akram, T., Sharif, M., Kadry, S., & Nam, Y. (2021). Computer Decision Support System for Skin Cancer Localization and Classification. *CMC-COMPUTERS MATERIALS & CONTINUA*, 68(1), 1041-1064.
- Kolachalama, V. B., Singh, P., Lin, C. Q., Mun, D., Belghasem, M. E., Henderson, J. M., ... & Chitalia, V. C. (2018). Association of pathological fibrosis with renal survival using deep neural networks. *Kidney international reports*, 3(2), 464-475.
- Krizhevsky, A., Sutskever, I., & Hinton, G. E. (2012). Imagenet classification with deep convolutional neural networks. *Advances in neural information processing systems*, 25, 1097-1105.
- Kuo, C. C., Chang, C. M., Liu, K. T., Lin, W. K., Chiang, H. Y., Chung, C. W., ... & Chen, K. T. (2019). Automation of the kidney function prediction and classification through ultrasound-based kidney imaging using deep learning. *NPJ digital medicine*, 2(1), 1-9.
- Långkvist, M., Jendeberg, J., Thunberg, P., Loutfi, A., & Lidén, M. (2018). Computer aided detection of ureteral stones in thin slice computed tomography volumes using Convolutional Neural Networks. *Computers in biology and medicine*, 97, 153-160.
- Lee, J. G., Jun, S., Cho, Y. W., Lee, H., Kim, G. B., Seo, J. B., & Kim, N. (2017). Deep learning in medical imaging: general overview. *Korean journal of radiology*, 18(4), 570.
- Li, J., Wang, P., Li, Y., Zhou, Y., Liu, X., & Luan, K. (2018, August). Transfer learning of pre-trained inception-V3 model for colorectal cancer lymph node metastasis classification. In *2018 IEEE International Conference on Mechatronics and Automation (ICMA)* (pp. 1650-1654). IEEE.
- Linkon, A. H. M., Labib, M., Bappy, F. H., Sarker, S., & Islam, M. S. (2020). Deep Learning Approach Combining Lightweight CNN Architecture with Transfer Learning: An

Automatic Approach for the Detection and Recognition of Bangladeshi Banknotes. *arXiv preprint arXiv:2101.05081*

Little, M. H., & Combes, A. N. (2019). Kidney organoids: accurate models or fortunate accidents. *Genes & Development*, *33*(19-20), 1319-1345.

Lu, T., Han, B., & Yu, F. (2021). Detection and classification of marine mammal sounds using AlexNet with transfer learning. *Ecological Informatics*, *62*, 101277.

Lundervold, A. S., & Lundervold, A. (2019). An overview of deep learning in medical imaging focusing on MRI. *Zeitschrift für Medizinische Physik*, *29*(2), 102-127.

Ma, F., Sun, T., Liu, L., & Jing, H. (2020). Detection and diagnosis of chronic kidney disease using deep learning-based heterogeneous modified artificial neural network. *Future Generation Computer Systems*, *111*, 17-26.

Marques, G., Agarwal, D., & de la Torre Díez, I. (2020). Automated medical diagnosis of COVID-19 through EfficientNet convolutional neural network. *Applied Soft Computing*, *96*, 106691.

Mayans, L. (2019). Nephrolithiasis. *Primary care*, *46*(2), 203-212.

Mazurowski, M. A., Buda, M., Saha, A., & Bashir, M. R. (2019). Deep learning in radiology: An overview of the concepts and a survey of the state of the art with focus on MRI. *Journal of magnetic resonance imaging*, *49*(4), 939-954.

McBee, M. P., Awan, O. A., Colucci, A. T., Ghobadi, C. W., Kadom, N., Kansagra, A. P., ... & Auffermann, W. F. (2018). Deep learning in radiology. *Academic radiology*, *25*(11), 1472-1480.

McCarthy, C. J., Baliyan, V., Kordbacheh, H., Sajjad, Z., Sahani, D., & Kambadakone, A. (2016). Radiology of renal stone disease. *International Journal of Surgery*, *36*, 638-646.

Mednikov, Y., Nehemia, S., Zheng, B., Benzaquen, O., & Lederman, D. (2018, July). Transfer representation learning using Inception-V3 for the detection of masses in mammography. In *2018 40th Annual International Conference of the IEEE Engineering in Medicine and Biology Society (EMBC)* (pp. 2587-2590). IEEE.

- Mesrabadi, H. A., & Faez, K. (2018, December). Improving early prostate cancer diagnosis by using Artificial Neural Networks and Deep Learning. In *2018 4th Iranian Conference on Signal Processing and Intelligent Systems (ICSPIS)* (pp. 39-42). IEEE.
- Milenkovic, U., & Albersen, M. (2019). Smoking and Men's Health. In *Effects of Lifestyle on Men's Health* (pp. 303-319). Academic Press.
- Monk, R. D., & Bushinsky, D. A. (2010). Nephrolithiasis and nephrocalcinosis. In *Comprehensive Clinical Nephrology* (pp. 687-701). Mosby.
- Monshi, M. M. A., Poon, J., & Chung, V. (2020). Deep learning in generating radiology reports: A survey. *Artificial Intelligence in Medicine*, 101878.
- Montalbo, F. J. P., & Alon, A. S. (2021). Empirical Analysis of a Fine-Tuned Deep Convolutional Model in Classifying and Detecting Malaria Parasites from Blood Smears. *KSI Transactions on Internet and Information Systems (TIIS)*, 15(1), 147-165.
- Motamedinia, P., Okhunov, Z., Okeke, Z., & Smith, A. D. (2015). Contemporary assessment of renal stone complexity using cross-sectional imaging. *Current urology reports*, 16(4), 18.
- Müftüoğlu, Z., Kizrak, M. A., & Yildirim, T. (2020, August). Differential Privacy Practice on Diagnosis of COVID-19 Radiology Imaging Using EfficientNet. In *2020 International Conference on INnovations in Intelligent SysTems and Applications (INISTA)* (pp. 1-6). IEEE.
- Nguyen, L. D., Lin, D., Lin, Z., & Cao, J. (2018, May). Deep CNNs for microscopic image classification by exploiting transfer learning and feature concatenation. In *2018 IEEE International Symposium on Circuits and Systems (ISCAS)* (pp. 1-5). IEEE.
- Nickolas, T. L., & Moe, S. M. (2019). Bone and Kidney. In *Basic and Applied Bone Biology* (pp. 375-386). Academic Press.
- Onthoni, D. D., Sheng, T. W., Sahoo, P. K., Wang, L. J., & Gupta, P. (2020). Deep Learning Assisted Localization of Polycystic Kidney on Contrast-Enhanced CT Images. *Diagnostics*, 10(12), 1113.

- Özkan, İ. N. İ. K., & Ülker, E. (2017). Derin öğrenme ve görüntü analizinde kullanılan derin öğrenme modelleri. *Gaziosmanpaşa Bilimsel Araştırma Dergisi*, 6(3), 85-104.
- Pacal, I., Karaboga, D., Basturk, A., Akay, B., & Nalbantoglu, U. (2020). A comprehensive review of deep learning in colon cancer. *Computers in Biology and Medicine*, 104003.
- Pahira, J. J., & Pevzner, M. (2007). Nephrolithiasis. In *Penn Clinical Manual of Urology* (pp. 235-257). WB Saunders.
- Parakh, A., Lee, H., Lee, J. H., Eisner, B. H., Sahani, D. V., & Do, S. (2019). Urinary stone detection on CT images using deep convolutional neural networks: evaluation of model performance and generalization. *Radiology: Artificial Intelligence*, 1(4), e180066.
- Park, J., Bae, S., Seo, S., Park, S., Bang, J. I., Han, J. H., ... & Lee, J. S. (2019). Measurement of glomerular filtration rate using quantitative SPECT/CT and deep-learning-based kidney segmentation. *Scientific reports*, 9(1), 1-8.
- Parmar, M. S. (2004). Kidney stones. *Bmj*, 328(7453), 1420-1424.
- Pérez, E., Reyes, O., & Ventura, S. (2021). Convolutional neural networks for the automatic diagnosis of melanoma: An extensive experimental study. *Medical image analysis*, 67, 101858.
- Pfau, A., & Knauf, F. (2016). Update on nephrolithiasis: core curriculum 2016. *American Journal of Kidney Diseases*, 68(6), 973-985.
- Pham, K. L., Dang, K. M., Tang, L. P., & Nguyen, T. N. (2020, November). GAN Generated Portraits Detection Using Modified VGG-16 and EfficientNet. In *2020 7th NAFOSTED Conference on Information and Computer Science (NICS)* (pp. 344-349). IEEE.
- Preuss, H. G. (1993). Basics of renal anatomy and physiology. *Clinics in laboratory medicine*, 13(1), 1-11.
- Quiñonez, Y., Lizarraga, C., Peraza, J., & Zatarain, O. (2019). Image recognition in UAV videos using convolutional neural networks. *IET Software*, 14(2), 176-181.

- Radhika, K., Devika, K., Aswathi, T., Sreevidya, P., Sowmya, V., & Soman, K. P. (2020). Performance analysis of NASNet on unconstrained ear recognition. In *Nature Inspired Computing for Data Science* (pp. 57-82). Springer, Cham.
- Rao, P. N. (2004). Imaging for kidney stones. *World journal of urology*, 22(5), 323-327.
- Reimer, R. P., Salem, J., Merkt, M., Sonnabend, K., Lennartz, S., Zopfs, D., ... & Hokamp, N. G. (2020). Size and volume of kidney stones in computed tomography: Influence of acquisition techniques and image reconstruction parameters. *European Journal of Radiology*, 132, 109267.
- Roy, A. D., & Islam, M. M. (2020, December). Detection of Epileptic Seizures from Wavelet Scalogram of EEG Signal Using Transfer Learning with AlexNet Convolutional Neural Network. In *2020 23rd International Conference on Computer and Information Technology (ICCIT)* (pp. 1-5). IEEE.
- Saba, L., Biswas, M., Kuppili, V., Godia, E. C., Suri, H. S., Edla, D. R., ... & Suri, J. S. (2019). The present and future of deep learning in radiology. *European journal of radiology*, 114, 14-24.
- Saxen, F., Werner, P., Handrich, S., Othman, E., Dinges, L., & Al-Hamadi, A. (2019, September). Face attribute detection with mobilenetv2 and nasnet-mobile. In *2019 11th International Symposium on Image and Signal Processing and Analysis (ISPA)* (pp. 176-180). IEEE.
- Schneider, M., Amann, R., & Mitsantisuk, C. (2021, March). Waste object classification with AI on the edge accelerators. In *2021 IEEE International Conference on Mechatronics (ICM)* (pp. 1-6). IEEE.
- Sharma, K., Rupprecht, C., Caroli, A., Aparicio, M. C., Remuzzi, A., Baust, M., & Navab, N. (2017). Automatic segmentation of kidneys using deep learning for total kidney volume quantification in autosomal dominant polycystic kidney disease. *Scientific reports*, 7(1), 1-10.
- Shirley, D. G., & Unwin, R. J. (2010). Renal physiology. In *Comprehensive clinical nephrology* (pp. 15-28). Mosby.

- Singh, P., Verma, A., & Alex, J. S. R. (2021). Disease and pest infection detection in coconut tree through deep learning techniques. *Computers and Electronics in Agriculture*, 182, 105986.
- Sorokin, I., Mamoulakis, C., Miyazawa, K., Rodgers, A., Talati, J., & Lotan, Y. (2017). Epidemiology of stone disease across the world. *World Journal of Urology*, 35(9), 1301-1320.
- Su, C., & Wang, W. (2020). Concrete Cracks Detection Using Convolutional NeuralNetwork Based on Transfer Learning. *Mathematical Problems in Engineering*, 2020.
- Sundar, K. S., Bonta, L. R., Baruah, P. K., & Sankara, S. S. (2018, March). Evaluating training time of Inception-v3 and Resnet-50,101 models using TensorFlow across CPU and GPU. In *2018 Second International Conference on Electronics, Communication and Aerospace Technology (ICECA)* (pp. 1964-1968). IEEE.
- Tahir, H., Iftikhar, A., & Mumraiz, M. (2021, February). Forecasting COVID-19 via Registration Slips of Patients using ResNet-101 and Performance Analysis and Comparison of Prediction for COVID-19 using Faster R-CNN, Mask R-CNN, and ResNet-50. In *2021 International Conference on Advances in Electrical, Computing, Communication and Sustainable Technologies (ICAECT)* (pp. 1-6). IEEE.
- Tajbakhsh, N., Shin, J. Y., Gurudu, S. R., Hurst, R. T., Kendall, C. B., Gotway, M. B., & Liang, J. (2016). Convolutional neural networks for medical image analysis: Full training or fine tuning?. *IEEE transactions on medical imaging*, 35(5), 1299-1312.
- Tanner, G. A. (2009). Kidney function. *Medical Physiology-Principles for Clinical Medicine*. 3rd ed. Philadelphia: Lippincott Williams and Wilkins, 391-418.
- Taş, M., & Yılmaz, B. (2021). Super resolution convolutional neural network based pre-processing for automatic polyp detection in colonoscopy images. *Computers & Electrical Engineering*, 90, 106959.
- Toğaçar, M., & Ergen, B. (2018, September). Deep learning approach for classification of breast cancer. In *2018 International Conference on Artificial Intelligence and Data Processing (IDAP)* (pp. 1-5). IEEE.

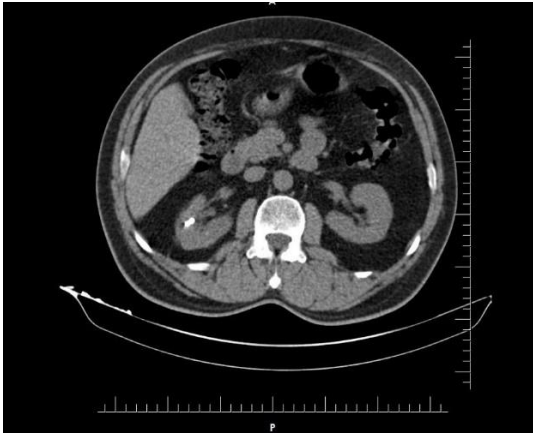
- Toraman, S., Tuncer, S. A., & Balgetir, F. (2019). Is it possible to detect cerebral dominance via EEG signals by using deep learning?. *Medical hypotheses*, *131*, 109315.
- Trong, V. H., Gwang-hyun, Y., Vu, D. T., & Jin-young, K. (2020). Late fusion of multimodal deep neural networks for weeds classification. *Computers and Electronics in Agriculture*, *175*, 105506.
- Vasanthselvakumar, R., Balasubramanian, M., & Sathiya, S. (2020). Automatic Detection and Classification of Chronic Kidney Diseases Using CNN Architecture. In *Data Engineering and Communication Technology* (pp. 735-744). Springer, Singapore.
- Vidyarthi, S. K., Singh, S. K., Tiwari, R., Xiao, H. W., & Rai, R. (2020). Classification of first quality fancy cashew kernels using four deep convolutional neural network models. *Journal of Food Process Engineering*, *43*(12), e13552.
- Vidyarthi, S. K., Singh, S. K., Xiao, H. W., & Tiwari, R. (2021). Deep learnt grading of almond kernels. *Journal of Food Process Engineering*, *44*(4), e13662.
- Waldman, S. D. (2019). *Atlas of Common Pain Syndromes E-Book*. Elsevier Health Sciences.
- Xuan, X., Han, R., Ji, S., & Ding, B. (2021, March). Research on Clothing Image Classification Models Based on CNN and Transfer Learning. In *2021 IEEE 5th Advanced Information Technology, Electronic and Automation Control Conference (IAEAC)* (Vol. 5, pp. 1461-1466). IEEE.
- Yamashita, R., Nishio, M., Do, R. K. G., & Togashi, K. (2018). Convolutional neural networks: an overview and application in radiology. *Insights into imaging*, *9*(4), 611-629.
- Yasaka, K., Akai, H., Kunimatsu, A., Kiryu, S., & Abe, O. (2018). Deep learning with convolutional neural network in radiology. *Japanese journal of radiology*, *36*(4), 257-272.
- Yıldırım, M. S., & Dandil, E. (2020). Automatic detection of multiple sclerosis lesions using Mask R-CNN on magnetic resonance scans. *IET Image Processing*, *14*(16), 4277-4290.

- Yuan, X., Shi, J., & Gu, L. (2020). A Review of Deep Learning Methods for Semantic Segmentation of Remote Sensing Imagery. *Expert Systems with Applications*, 114417.
- Zhang, Q., Wang, H., Yoon, S. W., Won, D., & Srihari, K. (2019). Lung nodule diagnosis on 3D computed tomography images using deep convolutional neural networks. *Procedia Manufacturing*, 39, 363-370.
- Zhao, S., Shadabfar, M., Zhang, D., Chen, J., & Huang, H. (2021). Deep learning-based classification and instance segmentation of leakage-area and scaling images of shield tunnel linings. *Structural Control and Health Monitoring*, e2732.
- Zheng, Y., Huang, J., Chen, T., Ou, Y., & Zhou, W. (2021). Transfer of Learning in the Convolutional Neural Networks on Classifying Geometric Shapes Based on Local or Global Invariants. *Frontiers in computational neuroscience*, 15, 15.

APPENDICES

APPENDIX
VARIOUS CT IMAGES

Appendix 1: With Kidney Stone CT Images



Appendix 2: Without Kidney Stone CT Images



Appendix 3: Turnitin Report

INBOX | NOW VIEWING: NEW PAPERS ▼

<input type="checkbox"/> Submit File		Online Grading Report Edit assignment settings Email non-submitters						
<input type="checkbox"/>	AUTHOR	TITLE	SIMILARITY	GRADE	RESPONSE	FILE	PAPER ID	DATE ▲
<input type="checkbox"/>	Özlem Sabuncu	Abstract	0% 	--	--		1607408403	16-Jun-2021
<input type="checkbox"/>	Özlem Sabuncu	Chapter 1	11% 	--	--		1607408811	16-Jun-2021
<input type="checkbox"/>	Özlem Sabuncu	Chapter 2	1% 	--	--		1607409185	16-Jun-2021
<input type="checkbox"/>	Özlem Sabuncu	Chapter 3	7% 	--	--		1607409430	16-Jun-2021
<input type="checkbox"/>	Özlem Sabuncu	Chapter 4	10% 	--	--		1607409781	16-Jun-2021
<input type="checkbox"/>	Özlem Sabuncu	Chapter 5. Results	0% 	--	--		1607410614	16-Jun-2021
<input type="checkbox"/>	Özlem Sabuncu	Chapter 6. Conclusion	0% 	--	--		1607410793	16-Jun-2021
<input type="checkbox"/>	Özlem Sabuncu	All thesis chapters	7% 	--	--		1607411779	16-Jun-2021

Appendix 4: Ethical Approval Document



K.K.T.C SAĞLIK BAKANLIĞI
DR BURHAN NALBANTOĞLU
DEVLET HASTANESİ



09/06/2021

Yakın Doğu Üniversite'sinde Öğretim Görevlisi Bülent Bilgehan'ın sorumlu araştırmacı olduğu
“Artificial Intelligence Model to Assist and Evaluate the Kidney Stone on CT Image” başlıklı
Yüksek Lisans Tezi 09/06/2021 tarihinde 32/21 proje kodu ile onaylanmıştır.

Gereği için bilgilerinize sunulur.


Etik Kurul Adına

Uzm. Dr. Ömer Taşargöl

İLETİŞİM
Tel: +90 392 22 85441
Fax: + 90 392 22 31899
Email: lbndtanitim@gmail.com